3

Molecular Interactions of Some Free Base Porphyrins with σ- and π-Acceptor Molecules

Abedien Zabardasti
Lorestan University,
Iran

1. Introduction

The basic structure of porphyrin consists of four pyrrole units linked by four methine bridges Fig. 1. The porphyrin macrocycle is an aromatic system containing 22π electrons, but only 18 of them are involved in any one delocalization pathway. It obeys Hückel's rule of aromaticity (4n+2 pi electrons) and has been shown by X-ray crystallography to be planar.

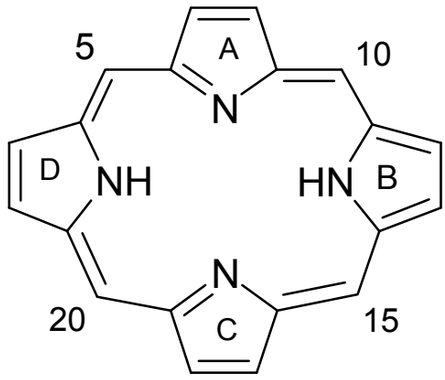

Fig. 1. Structure of free base porphyrin

1.1 ^{1}H NMR spectra of porphyrins

The aromatic character of porphyrins can also be seen by NMR spectroscopy. Studies performed in the last decades demonstrated that ^{1}H NMR spectra are very informative and adequately reflect the structural features of porphyrins.[1] The presence of the extended delocalized π-electron system of the porphyrin macrocycle gives rise to a strong ring current in the molecules placed in the magnetic field. The ring current causes anisotropic shielding of the protons located in the field of its action and (together with the diamagnetic component of paired σ-electrons) leads to a substantial shift of their signals in the ^{1}H NMR spectra. It can be stated that the ring current and the aromaticity of porphyrins change in a similar way in response to the analogous changes in the molecular structure of the porphyrin and the medium, which is most clearly seen on comparison of the spectra of porphyrins and their precursors. Due to the anisotropic effect from the porphyrin ring

current, the NMR signals for the deshielded meso protons (protons on the bridging methine carbons) show up at low field, whereas the signals for the shielded protons on the inner nitrogen atoms show up at very high field. Theoretical analysis of the ^{1}H NMR spectra shows that the positions of the signals for the protons of porphyrins are determined primarily by the strength of ring π-electron currents (the macrocyclic current enclosing the molecule as a whole and local currents localized in the pyrrole nuclei (Fig. 2a,b). It should be noted that the macrocyclic current (Fig. 2a) possesses the major `bed' corresponding to the main 18-membered contour of conjugation and `arms' formed by the semi-isolated $C_{(\beta)}$-$C_{(\beta)}$ bonds in the pyrrolenine nuclei.

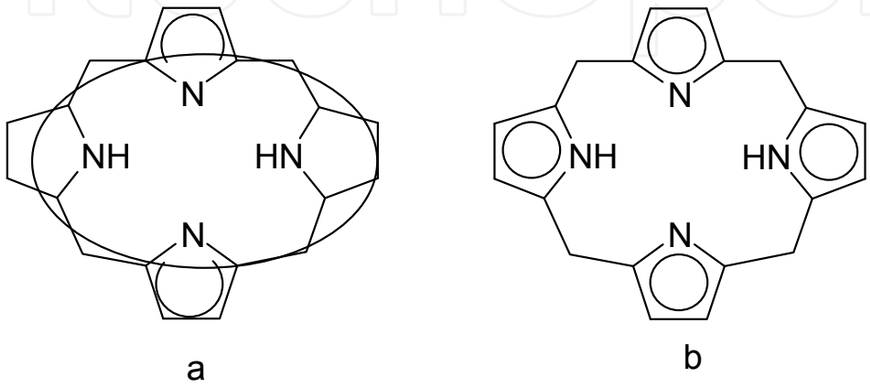

Fig. 2. Schematic representation of the circuits of the ring π-electron currents in the porphyrin molecule; (a) the macrocyclic current, (b) local currents.[1]

The protons at the β and meso positions are exocyclic with respect to the macrocyclic and local pyrrole currents and experience the deshielding influence of the latter. The signals for these protons are observed at low field (at δ from 9.7 to 11.2 ppm for the meso-protons and at δ from 8.5 to 9.9 ppm for the β-protons, Table 1). The protons of the NH groups are exocyclic with respect to the local ring currents and endocyclic with respect to the macrocyclic current. Undoubtedly, the shielding effect of the latter prevails and the signals for the protons of the NH groups are observed at very high field (at δ from -1.4 to -4.4 ppm). [1]

Compound	δ N-H	δ $H_{m,p}$	δ H_o	δ H_β	δ OCH_3 ,δ CH_3
H_2TPP	-2.71	7.81	8.26	8.87	-
H_2T(4-Cl)PP	-2.86	7.75	8.14	8.85	-
H_2T(4-CH_3)PP	-2.77	7.56	8.11	8.86	2.71
H_2T(4-CH_3O)PP	-2.82	7.23	8.07	8.79	3.95

Table 1. ^{1}H NMR chemical shift (δ/ppm) of the free base tetraarylporphyrins relative to $CHCl_3$.

The β-hydrogen atoms of the pyrrole and pyrrolenine fragments are in principle nonequivalent. However, rapid (within the NMR time scale) transformations occur at room temperature and the signals for the β-protons are averaged. Two different peaks corresponding to resonance absorption of the energy by the protons of the β-CH groups of the pyrrole and pyrrolenine fragments can be observed at low temperature, -80 °C. [1,2]

On going from H_2P to H_4P^{2+} it would expect that the signals for the protons of the NH groups in the ^1H NMR spectrum would be shifted downfield upon protonation of porphin. However, the signals are shifted upfield by ~0.7 ppm. Simultaneously, the signals for the β- and meso-protons are shifted downfield. This character of the spectral changes indicates that protonation of porphin leads to a substantial increase in the strength of the magnetic field induced by the macrocyclic ring current.

Protonation of porphin is accompanied by a change in the geometric structure of the molecule. The $C_{(\alpha)}$-NH-$C_{(\alpha)}$ fragments in the initial porphin are planar and the nitrogen atoms are sp^2-hybridized. In the protonated porphin, these fragments adopt a pyramidal structure (the nitrogen atoms have nearly sp^3 hybridization) and the degree of involvement of the nitrogen atoms in conjugation with the α-carbon atoms is substantially reduced. This fact is confirmed by an increase in the $C_{(\alpha)}$-N bond length observed upon protonation of porphin. The above-mentioned rearrangements lead to a change in the contour of macrocyclic conjugation. In the case of protonated porphin, this conjugation is realized primarily along the outer contour of the molecule. Therefore, protonation causes an increase in the diameter of the conjugation ring resulting in upfield shifts of the signals for the internal protons and downfield shifts of the signals for the external protons. In the case of β-alkyl substitution in porphin (on going to octaethylporphin and ethioporphyrin), the signals for the protons of the NH groups and the signals for the meso-protons are shifted downfield and upfield, respectively. Analogous, but more pronounced, changes are observed in the presence of a substituent in the meso position. It should be noted that the introduction of both electron-donating (meso-tetra-iso-butyl- and meso-tetra-n-pentylporphyrin) and electron-withdrawing (tetraphenylporphyrin and its derivatives) substituents gives the same results, viz., the signals for β-protons and for the protons of the NH groups are shifted upfield and downfield, respectively. It seems likely that the introduction of substituents both at the β- and meso positions leads to reduction in the strength of the aromatic macrocyclic current regardless of the electronic nature of the substituent.

The currents in the porphyrin molecule are substantially affected by complex formation.[1] The higher the degree of covalence of the N-H bond, the larger the decrease in the ring current due to the presence of the coordinated metal atom. Coordination to the medium-sized M^{2+} cations (M =Mg, Zn, Cd, Ni or Pd) is accompanied by upfield shifts of the signals for the meso-protons (the ring current is reduced). In the spectra of the complexes in which the M^{2+} metal ion deviates from the plane due to its large radius and weak coordination interactions (M =Sn or Pb) or in the spectra of the complexes with the M^{3+} or M^{4+} ions in which the metal atom deviates from the plane of the macrocycle under the action of the extra ligands, the signals for the meso-protons are shifted downfield relative to those in the spectra of the porphyrin ligand. These shifts may be due to an increase in the ring current. However, this effect is insignificant and depends on the nature of the ions serving as the extra ligands.[1]

1.2 Electronic absorption spectra of porphyrins

Electronic absorption spectra of porphyrins are very characteristic and contain one intense band in the near-ultraviolet region of the spectrum around 390-425 nm depending on whether the porphyrin is β- or meso-substituted with $\varepsilon > 2 \times 10^5$, the Soret band or B band, followed by four low-intensity absorption bands at higher wavelengths (480 to 650 nm) in

the visible region (Q Bands), see Fig. 3 and Table 2. These absorptions giving rise to striking colours of porphyrins. Thus, free base porphyrins have four Q bands, denoted by increasing wavelength as IV, III, II, and I. The commonly accepted classification of these bands is as follows. The bands I and III in the visible region of the spectrum (Fig. 3) belong to quasi-forbidden electron transitions, whereas the bands II and IV are of electronic-vibrational origin, i.e., are vibrational satellites of the bands I and III, respectively. Although possessing a number of common features, the spectra of porphyrins show substantial variations, which reflect the changes in the molecular structure and the effect of the solvent.

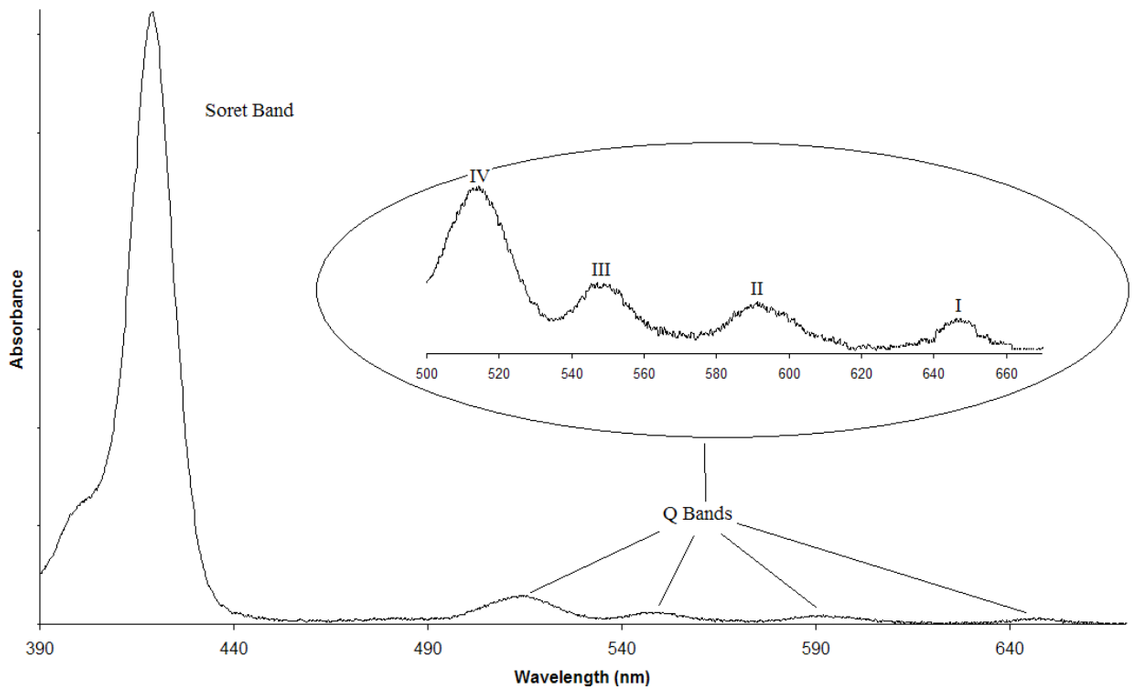

Fig. 3. Typical UV-vis absorption spectrum of a porphyrin.

Compound	Wavelength (nm)				
H_2TPP	417	514	549	589	646
$H_2T(4\text{-}Cl)PP$	418	514	550	590	646
$H_2T(4\text{-}CH_3)PP$	419	516	553	591	649
$H_2T(4\text{-}CH_3O)PP$	421	518	555	594	649

Table 2. UV-vis absorptions λ ($CHCl_3$/nm) of the free base tetraarylporphyrins.

According to the universally accepted concepts, light absorption is accompanied by excitation of the porphyrin molecule and the characteristic features of the absorption spectrum are determined by transitions of the π-electrons between two higher occupied and two lower unoccupied orbitals, the four-orbital Platt - Gouterman model.[1]

The intensity ratio of the absorption bands in the spectra of porphyrins depends on their structures in a peculiar fashion. When the relative intensities of these bands are such that IV > III > II > I, then the spectrum is said to be ethio-type after the ethioporphyrins in which

the β-substituents are all alkyl groups, Fig. 4a. In practice, the ethio-type Q band spectrum is found in meso-tetraphenylporphyrin, ethio-porphyrin and all porphyrins in which six or more of the β-positions are substituted with groups without π-electrons, e.g. alkyl groups. For porphyrins characterized by the rhodo-type of the spectra (after rhodoporphyrin XV) the following sequence III > IV > II > I is realized, Fig. 4b. Among the latter compounds are rhodoporphyrin and other porphyrins containing an electron-withdrawing substituent (COOH, NO_2, Cl, etc.) in the pyrrole fragment. The rhodo-type spectrum has a "rhodoflying" or "reddening" effect on the spectrum by shifting it to longer wavelength. Phylloporphyrin and other porphyrins containing one or two meso-substituents are characterized by the phyllo type of the spectrum (IV > II > III > I), Fig. 4c. Chlorin, tetrabenzoporphyrin and phthalocyanine give characteristic spectra of their own. In their spectra, the long-wavelength band I has the maximum intensity. Variations of the peripheral substituents on the porphyrin ring often cause minor changes to the intensity and wavelength of these absorptions. Protonation of two of the inner nitrogen atoms or insertion of a metal into the porphyrin cavity also changes the visible absorption spectrum. These absorptions can often be very helpful in determining certain features on a porphyrin.

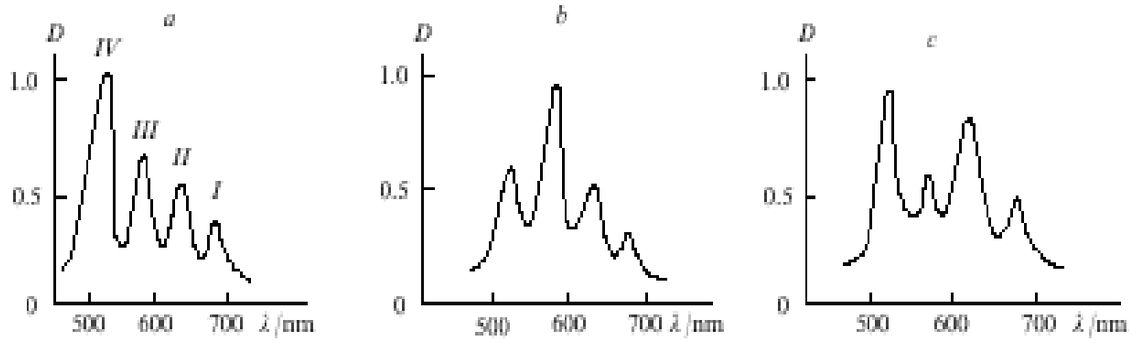

Fig. 4. Basic types of electronic absorption spectra of ethio- (a), rhodo- (b) and phylloporphyrins (c).

The meso-tetrasubstituted porphyrins are characterized by a distorted ethio type of spectra with rather large (25 - 40 nm) red shifts of the bands. The introduction of various substituents at the para positions of the phenyl rings of meso-tetraphenyl-porphyrin causes red shifts of the absorption bands in the visible region of the spectra. A comparison of the spectra of tetraphenylporphyrin and its para-substituted derivatives demonstrated that the intensities of the electron transition bands (I and III) rise as the electron-donating properties of the substituents increase. Simultaneously, the intensities of the vibrational bands (II and IV) are diminished.[3] The ethio type of the spectrum of tetraphenylporphyrin is distorted because the band I becomes more intense than the band II.

The presence of electron-donating substituents at the meta positions also leads to red shifts of the bands, the intensities of the vibrational bands being increased, while the intensities of the electron transition bands remaining virtually unchanged. The spectra of ortho-substituted tetraphenylporphyrins are characterized by lower intensities of the electron transition bands compared to those observed in the electronic absorption spectrum of tetraphenylporphyrin. In some cases, this gives rise to the spectra of the phyllo type, for example, in the case of tetra(2-halogenophenyl)porphyrins and, particularly, in the case of tetrakis(2,6-dihalogenophenyl)porphyrins.

The absorption spectra are also dependent on the solvent. Thus, the bands in the electronic absorption spectra of substituted meso-tetraphenylporphyrins are shifted redally and the intensities of the electron transition bands grow on going from nonpolar hexane to polar pyridine.

On going from porphyrin to metalloporphyrin, the symmetry of the planar macrocyclic fragment (of the π-electron cloud of the macrocycle) increases due to which the spectrum is simplified. The Soret band changes only slightly upon complex formation. The visible region of the spectra of metal complexes has two absorption bands, viz., the band I corresponding to the electron transition and the band II corresponding to the electronic-vibrational transition.

1.3 Sitting-Atop (SAT) complexes

A particularly attractive idea in the kinetic and mechanism of metalation of free base porphyrins is that of the Sitting-Atop (SAT) complexes.[4,5] In 1960, Fleischer and Wang [4] first proposed the so-called Sitting-Atop complexes of the protoporphyrin dimethyl ester with metal ions in chloroform on the basis of visible spectra, infrared spectra and composition of the SAT complex. According to the SAT idea the metalation of free base porphyrin begins with a preequilibrium step involving partial bonding of the metal ion to two of pyrrolenine nitrogens to form an intermediate, so-called Sitting-Atop complex. In this intermediate two protons on the pyrrole nitrogens still remain, $M(H_2P)^{2+}$ (Eq. 1). Then the overall metalation reaction will consist of at least two steps, i.e., the coordination step of two pyrrolenine nitrogens to form an intermediate, so-called Sitting-Atop complex, and the deprotonation step of the SAT complex to form the metalloporphyrin, as shown by following Equations, respectively:

$$M^{n+} + H_2P \rightleftharpoons M(H_2P)^{2+} \quad (1)$$

$$M(H_2P)^{2+} \rightleftharpoons M(P)^{(n-2)+} + 2H^+ \quad (2)$$

The existence of the SAT complex could explain the experimental kinetics of the metalation for several porphyrins in N,N-dimethylformamide (DMF),[6-8] acetic acid,[9] dimethyl sulfoxide (DMSO),[10] and H_2O.[11,12] However, the formation constant of the SAT complex was reported as being on the order of 10^2 -10^4 mol $^{-1}$dm^3 for Cu(II) and Zn(II) ions in DMF.[13,14]

S. Funahashi et al.[15,16] have been succeeded to direct detection of SAT complexes of some tetraarylporphyrin with the Cu(II) ion in the acetonitrile as a solvent. Structural characterization of the Cu(II)-SAT complex in AN by the ^{1}H NMR and EXAFS methods clarified that two pyrrolenine nitrogens coordinate to the equatorial sites of the Cu(II) ion and H_2TPP act as a bidentate ligand.

They proposed the following overall mechanism for the metalation reaction of H_2tpp with an octahedrally solvated metal(II) ion (MS_6^{2+}) in the conventional basic solvent (S); which resolved into Eqs 3-8: the deformation of the porphyrin ring (eq 3), the outer-sphere association (eq 4), the rate-determining exchange of a coordinated solvent molecule with a first pyrrolenine nitrogen (eq 5), the chelate ring closure to form the SAT complex (eq 6), the first deprotonation on the pyrrole nitrogen in the SAT complex by the basic solvent molecule (S) (eq 7), and the second deprotonation to form the metalloporphyrin (eq 8),

$$H_2tpp \overset{K_D}{\rightleftharpoons} H_2tpp \quad (3)$$

$$H_2tpp + MS_6^{2+} \overset{K_{OS}}{\rightleftharpoons} H_2tpp{*}\,MS_6^{2+} \quad (4)$$

$$H_2tpp{*}\,MS_6^{2+} \underset{k_{-1}}{\overset{k_1}{\rightleftharpoons}} MS_5(H_2tpp)^{2+} + S \quad (5)$$

$$MS_5(H_2tpp)^{2+} \overset{K_{RC}}{\rightleftharpoons} MS_p(H_2tpp)^{2+} + (5\text{-}p)S \quad (6)$$

$$MS_p(H_2tpp)^{2+} + S \overset{K_{-H1}}{\rightleftharpoons} MS_q(H_2tpp)^{+} + HS^{+} + (p\text{-}q)S \quad (7)$$

$$MS_q(H_2tpp)^{+} + S \overset{K_{-H2}}{\rightleftharpoons} MS_r(tpp) + HS^{+} + (q\text{-}r)S \quad (8)$$

Where, $p \leq 4$, $q \leq p - 1$, and $r \leq 2$. In the case of M = Cu, S = AN, and S = py, it was determined by fluorescent XAFS measurements that p = 4 and r = 0.

There are numerous reports on thermodynamic parameters of SAT complex of free base porphyrins with bivalent metal ions. M. Tanaka et al.[7] have studied the incorporation of Cu(II), Zn(II) and Cd(II) in the free base H_2TPP in DMF. They suggested a preequilibrium between metal ions and H_2TPP prior to metal insertion and proton release. Their values of K were 1.6×10^4 M^{-1} for Cu(II), 7.2×10^2 M^{-1} for Zn(II), and no kinetic evidence for complex formation was found for Cd(II). Pasternack's group[11] kinetically found a K 5 M^{-1} for Cu(II)-H_2TPP reaction in DMSO. P. Hambright and L.R. Rabinson [8] have studied the kinetic of Zn(II) incorporation into free base porphyrins in DMF as solvent. They obtained the following values of K for Zn(II) SAT complexes with tetraphenylporphyrin, tetrakis (2,6-diflourophenyl)porphyrin, tetra(4-aminophenyl)porphyrin, tetrakis(4-N,N-dimethylaminophenyl) porphyrin, and tetra(4-hydroxyphenyl)porphyrin, 12.3×10^3, 2.8×10^3, 7.7×10^3, 6.0×10^3, and 9.5×10^3 M^{-1}, respectively. This short review on Sitting-Atop complexes illustrated that these intermediates have been interest from 1960.

Concerning non-basicity and noncoordinating properties of some solvents such as chloroform and dichloromethane make them suitable solvents for obtaining SAT complex as a solid product. On the other hand, molecular Lewis acids such as organotin(IV) halides because of some special properties, i.e., a high solubility in noncoordinating solvents, a suitable stability in solution, a good tendency to adduct formation, and enough stability of their adducts for characterization are remarkable candidates for determination of SAT complexes.

1.4 Molecular adducts

1.4.1 Molecular adducts of organotin(IV) halides with free base *meso*-tetraarylporphyrins [17-23]

General procedure

On excess addition of organotin(IV) halides to a purple solution of free base tetraarylporphyrin in dry chloroform, its color changed to green. Evaporation of the solvent

at room temperature results to shiny green powdery product. Elemental analysis, electronic absorptions spectra and ^{1}H NMR spectroscopy were used to characterization of product.

1.4.1.1 Molecular adducts of dimethyltin(IV) dichloride with free base meso-tetraarylporphyrins, [$(Me_2SnCl_2)_2H_2T(4\text{-}X)PP$] [22]

Table 3 shows the elemental analyses for adducts obtained from interaction of some organotin(IV) halides with free base tetraphenylporphyrin derivatives. These data are in agreement with a composition 2:1 of adducts in the solid state. On the basis of spectroscopic measurements a Sitting-Atop structure was suggested for these adducts. Of course, stoichiometry of adduct might differ in the solution from the solid product.

1.4.1.2 UV-Visible analysis

Interaction of tetraphenylporphyrins with sigma- and pi-acceptor species lead to green products that their UV-Vis spectra are comparable with diacid form of corresponding porphyrin. In the electronic absorption spectra of the diacid form of free base H_2TPP the intensity of band I is greater than band II. All the bands in the UV-visible spectra of H_4TPP^{2+} are shifted 20-40 nm to the red.[24-26] This is interpreted to be evidence of increased resonance interaction of the phenyl rings with the porphyrin nucleus in going from the free base to it's diacid form, which would be allowed by the tilting of the pyrroles observed in the solid state. The phenyl ring angle with plane of porphyrin in H_2TPP is within 60-85 ^{o}, which this angle reduces to 21 ^{o} in H_4TPP^{2+}. The red shift in H_4TPP^{2+} (UV-Vis H_4TPP^{2+} (in CH_2Cl_2), 439, 602, 655 nm) relative to H_2TPP is consistent with the structural observation that the phenyl rings in H_4TPP^{2+} were more coplanar with the porphyrin nucleus than free base H_2TPP. With this coplanarity some resonance interaction of these rings with porphyrin nucleus is thus allowed, and may be the reason why the diacid form of H_2TPP is green in solution. Similar situations were observed for interaction of free base $H_2T(4\text{-}X)PPs$ with organotin(IV) halide Lewis acids. During these interactions original peaks of free base $H_2T(4\text{-}X)PPs$ (Soret band and Q band) were slowly changed to two new peaks which their position show about 20-40 nm red shift relative to the band V (Soret band) and the band I (of Q band) of free base $H_2T(4\text{-}X)PPs$, Table 4. It seems that deformation of porphyrin structure during its interaction with various acceptor species is similar to deviations of porphyrins skeleton in porphyrin diacids $H_4T(4\text{-}X)PP^{2+}$ (Table 4). In the thermodynamic studies section we will review the spectral variation of free base meso-tetraarylporphyrins upon formation of their adducts.

Investigating the effect of adduct formation on the electronic absorption spectra of the free base porphyrins, the red shifts of absorption bands were observed on going from free bases to adducts. This is due to an increased in the resonance interaction of the peripheral phenyl rings with the porphyrin nucleus. The amounts of shift vary from 28 to 36 nm, depending on *the kind of acceptor, for the Soret band. In $(MeSnBr_3)_2H_2TPP$, Soret band (448 nm) and Q band I (666 nm) with 30 and 20 nm shift, respectively, we find the greatest red shift in the H_2TPP adducts. Also $(MeSnBr_3)_2H_2T(4\text{-}Cl)PP$ with 34 and 25, in $(MeSnBr_3)_2H_2T(4\text{-}CH_3)PP$ with 31 and 29 nm, in $(MeSnBr_3)_2H_2T(4\text{-}CH_3O)PP$ with 35 and 46 nm red shift they have the greatest red shift in the corresponding adducts. It indicates that there is a direct relation between the acceptor property of the organotin(IV) halide Lewis acid and the red shift of the electronic absorption spectra of the coordinated porphyrin. Also, the red shifts of the absorption bands of the coordinated tetraarylporphyrins depend on the substituents at the para positions of their phenyl rings. By*

Adduct	Found			Calculated			Adduct	Found			Calculated		
	C	H	N	C	H	N		C	H	N	C	H	N
$(Me_2SnCl_2)_2H_2TPP$	52.15	3.89	4.98	54.60	3.98	5.30	$(Ph_2SnCl_2)_2H_2TPP$, $\underline{0.23CHCl_3}$	61.57	3.91	3.98	61.62	3.81	4.21
$(Me_2SnCl_2)_2H_2T(4\text{-}Cl)PP$	49.16	3.25	4.95	48.30	3.18	4.69	$(Ph_2SnCl_2)_2H_2T(4\text{-}Cl)PP$,$\underline{0.45CHCl_3}$	55.10	3.37	3.18	55.02	3.14	3.75
$(Me_2SnCl_2)_2H_2T(4\text{-}CH_3)PP$	59.10	4.72	5.30	56.87	4.50	5.04	$(Ph_2SnCl_2)_2H_2T(4\text{-}CH_3)PP$,$\underline{0.6CHCl_3}$	60.85	4.01	3.82	60.97	4.13	3.92
$(Me_2SnCl_2)_2H_2T(4\text{-}CH_3O)PP$	51.13	4.46	4.50	53.40	4.25	4.77	$(Ph_2SnCl_2)_2H_2T(4\text{-}CH_3O)PP$,$\underline{0.6CHCl_3}$	58.30	3.76	3.35	58.35	3.95	3.75
$(Et_2SnCl_2)_2H_2TPP$	55.46	4.44	4.79	56.17	4.50	5.04	$(Ph_2SnBr_2)_2H_2TPP$	55.60	3.80	4.20	55.19	3.38	3.78
$(Et_2SnCl_2)_2H_2T(4\text{-}Cl)PP$	49.18	3.70	4.29	49.96	3.68	4.48	$(Ph_2SnBr_2)_2H_2T(4\text{-}Cl)PP$	50.60	3.20	3.60	50.49	2.84	3.46
$(Et_2SnCl_2)_2H_2T(4\text{-}CH_3)PP$	56.86	4.73	4.55	57.59	4.97	4.80	$(Ph_2SnBr_2)_2H_2T(4\text{-}CH_3)PP$,$\underline{0.8CHCl_3}$	53.50	3.90	3.30	53.58	3.63	3.43
$(Et_2SnCl_2)_2H_2T(4\text{-}CH_3O)PP$	55.51	4.98	4.56	54.60	4.71	4.55	$(Ph_2SnBr_2)_2H_2T(4\text{-}CH_3O)PP$,$\underline{CHCl_3}$	50.70	3.70	3.00	50.98	3.46	3.25
$(Bu_2SnCl_2)_2H_2TPP$	55.79	4.96	4.63	58.97	5.41	4.59							
$(Bu_2SnCl_2)_2H_2T(4\text{-}Cl)PP$	51.88	3.70	4.29	52.91	4.56	4.12							
$(Bu_2SnCl_2)_2H_2T(4\text{-}CH_3)PP$	58.75	5.45	4.63	60.15	5.80	4.39							
$(Bu_2SnCl_2)_2H_2T(4\text{-}CH_3O)PP$	55.65	5.49	3.83	57.28	5.52	4.18							
$(MeSnCl_3)_2H_2TPP$	44.16	2.25	4.15	44.74	2.56	4.54							
$(MeSnCl_3)_2H_2T(4\text{-}Cl)PP$	49.75	3.09	4.88	50.37	3.28	5.11							
$(MeSnCl_3)_2H_2T(4\text{-}CH_3)PP$	51.62	4.12	4.63	52.10	3.82	4.86							
$(MeSnCl_3)_2H_2T(4\text{-}CH_3O)PP$	48.53	4.04	4.20	49.35	3.62	4.61							

Table 3. Elemental analysis of $[(Me_2SnCl_2)_2H_2T(4\text{-}X)PP]$ adducts

increasing electron donation of the *para*-substituents on the phenyl rings greater red shift were observed for the absorption bands in the visible spectra of tetraarylporphyrin during adduct formation. Also the electronic absorption spectra of adducts are indicating that the intensity of the electron transition band I of the adducts rises as the electron donation properties of the substituents increase.

Considering λ_{max} of the electronic absorption bands (Soret and band I) of adducts it might be pointed out that the kind of acceptor have a minor effect on the position of the adduct bands. It seems positions of these bands depend on distortion and tilting of the porphyrin plane, which occurred during formation of 1:1 adduct for different acceptors. Therefore the kind of acceptor and also entering the second acceptor species isn't accompanied with a significant replacement in the position of the adduct bands. The same statement can be discussed for position of the isosbestic points of free base porphyrins adducts with various acceptors. The effect of distortion of porphyrin structure on electronic absorption bands and ^{1}H NMR chemical shift of various free base porphyrin protons will be better understood by comparison of electronic absorption spectra of 5,10,15,20-tetrabutylporphyrin as a planar free base porphyrin [UV-vis (CH_2Cl_2): Soret band (417 nm) and Q bands (520, 555, 600, 659 nm); ^{1}H NMR: N-H (-2.61 ppm) and H_β(9.45 ppm)] with 5,10,15,20-tetrakis(tert-butyl)porphyrin as a severely ruffled (distorted) free base porphyrin [Soret band (446 nm) and Q bands (552, 596, 628, 691 nm); ^{1}H NMR: N-H (1.52 ppm) and H_β(9.08 ppm)]. This example finely shows that the observed red shift mainly resulted upon distortion of porphyrin structure.

1.4.2 Molecular adducts of methyltin(IV) tribromide with free base *meso*-tetraarylporphyrins, $[(MeSnBr_3)_2H_2T(4\text{-}X)PP]$: [21]

On addition of methyltin(IV) tribromide to a solution of free base tetraarylporphyrins in dry chloroform its purple color changed to green, the electronic absorption spectra of adducts are given in the Table 4.

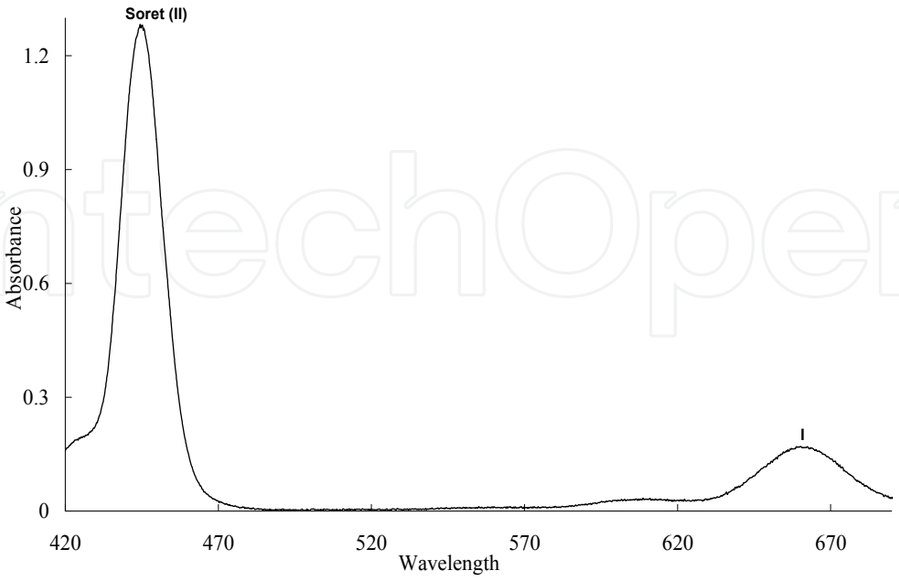

Fig. 5. Typical electronic absorption spectra of porphyrin diacid (H_4TPP^{2+}) and porphyrin molecular adducts $[(R_nSnCl_{4-n})_2H_2TPP]$.

Compound	λ(nm)		Compound	λ (nm)	
$(Me_2SnCl_2)_2H_2TPP$	445	660	$(Ph_2SnCl_2)_2H_2T(4\text{-}Cl)PP$	448	664
$(Me_2SnCl_2)_2H_2T(4\text{-}Cl)PP$	447	664	$(Ph_2SnBr_2)_2H_2T(4\text{-}Cl)PP$	452	668
$(Me_2SnCl_2)_2H_2T(4\text{-}CH_3)PP$	448	672	$(Ph_2SnCl_2)_2H_2TPP$	444	660
$(Me_2SnCl_2)_2H_2T(4\text{-}CH_3O)PP$	453	690	$(Ph_2SnBr_2)_2H_2TPP$	448	662
$(Et_2SnCl_2)_2H_2TPP$	444	660	$(Ph_2SnCl_2)_2H_2T(4\text{-}CH_3)PP$	448	670
$(Et_2SnCl_2)_2H_2T(4\text{-}Cl)PP$	448	664	$(Ph_2SnBr_2)_2H_2T(4\text{-}CH_3)PP$	450	676
$(Et_2SnCl_2)_2H_2T(4\text{-}CH_3)PP$	447	670	$(Ph_2SnCl_2)_2H_2T(4\text{-}CH_3O)PP$	453	688
$(Et_2SnCl_2)_2H_2T(4\text{-}CH_3O)PP$	453	688	$(Ph_2SnBr_2)_2H_2T(4\text{-}CH_3O)PP$	456	694
$(Bu_2SnCl_2)_2H_2TPP$	444	660	$(MeSnBr_3)_2H_2TPP$	448	666
$(Bu_2SnCl_2)_2H_2T(4\text{-}Cl)PP$	448	664	$(MeSnBr_3)_2H_2T(4\text{-}Cl)PP$	452	670
$(Bu_2SnCl_2)_2H_2T(4\text{-}CH_3)PP$	448	670	$(MeSnBr_3)_2H_2T(4\text{-}NO_2)PP$	458	662
$(Bu_2SnCl_2)_2H_2T(4\text{-}CH_3O)PP$	453	688	$(MeSnBr_3)_2H_2T(4\text{-}CH_3)PP$	450	676
$(MeSnCl_3)_2H_2T(4\text{-}Cl)PP$	452	670	$(MeSnBr_3)_2H_2T(4\text{-}CH_3O)PP$	456	696
$(MeSnCl_3)_2H_2TPP$	448	666	$H_4T(4\text{-}Cl)PP^{2+}$	444	661
$(MeSnCl_3)_2H_2T(4\text{-}CH_3)PP$	450	676	H_4TPP^{2+}	442	659
$(MeSnCl_3)_2H_2T(4\text{-}CH_3O)PP$	454	690	$H_4T(4\text{-}CH_3)PP^{2+}$	446	672
			$H_4T(4\text{-}CH_3O)PP^{2+}$	453	695

Table 4. UV-vis absorptions λ ($CHCl_3$/nm) of $[(Me_2SnCl_2)_2H_2T(4\text{-}X)PP]$ adducts.

1.4.2.1 ^{1}H NMR analysis

Up to getting a detailed description of ^{1}H NMR spectra of adducts, an overview on ^{1}H NMR of Cu(II)-SAT complex, S. Funahashi et al.,[16] will be informative. S. Funahashi et al. have studied the ^{1}H NMR variation of H_2TPP during a reaction between Cu(II) ion and H_2TPP in acetonitrile for detecting the SAT complex by spectroscopic method.

Table 5 summarized the chemical shift values of SAT complex together with the reported values for H_2TPP.[27, 28] Although the SAT complex contains the paramagnetic Cu(II) ion having $S = 1/2$, the β-pyrrole protons have been clearly observed. In the ^{1}H NMR spectra signal of the N-H protons in the SAT complex was clearly observed at -2.05 ppm relative to TMS strongly indicated that the N-H protons remain in the SAT complex ($Cu(H_2TPP)^{2+}$). In contrast to the case of H_2TPP, two kinds of β-protons for the SAT complex were observed with a ratio of 1:1, which had twice the area of the peak for N-H protons. The peaks, one a singlet and the other a doublet, were attributed to the protons in the pyrrolenine group coordinated and in the pyrrole group not coordinated to the Cu(II) ion, respectively. A similar splitting was reported for H_2TPP at the low temperature of -80 °C, because the N-H

Solute	N-H	Phenyl (H_o)	Phenyl ($H_{m,p}$)	Pyrrole (H_β)
H_2TPP	-2.87 (s)	7.80-7.87 (m)	8.22-8.25 (m)	8.85 (s)
$Cu(H_2TPP)^{2+}$	-2.05 (s)	7.31-7.50 (m)	8.10-8.12 (m)	8.66(d),8.77(s)

Table 5. Values of chemical shift (δ; relative to TMS/ppm) for H_2TPP and it's SAT complex in CD_3CN.

tautomerism at such a low temperature was frozen where the signal of the β-pyrrole protons of the pyrrole groups with N-H protons was observed at a lower field relative to that of the pyrrolenine groups without the N-H protons. The opposite trend in chemical shift was, however, observed for the SAT complex, i.e., the doublet peak assigned to the β-pyrrole protons appears at a higher field (see Fig. 6). This indicates that the two pyrrolenine nitrogens without an N-H proton bind to the paramagnetic Cu(II) ion, because the dipole-dipole and scalar coupling interactions with the paramagnetic ion lead to their downfield shift.[15,16] Furthermore, the peak for N-H protons was shifted downfield relative to that of H_2TPP. This is ascribed to both the distortion of the porphyrin ring and the dipole-dipole interaction with the paramagnetic ion. Because the N-H protons in H_2TPP are highly shifted to the upper field due to the ring current of the planar porphyrin ring, the distortion of the porphyrin ring in the SAT complex then leads to the downfield shift. The ^1H NMR spectrum determines a symmetrical structure with pyrrolenine nitrogens coordinating to the Cu(II) ion.

We used the low temperature ^1H NMR (-30 ^oC) to study the molecular interaction of free base porphyrins with organotin(IV) halides. ^1H NMR spectra of free base porphyrins undergo considerable variations during these interactions.

Data given in Table 6 are indicating that by interaction of free bases $H_2T(4\text{-}X)PP$ with R_nSnX_{4-n} the original bands of N-H, H_{β}, H_o, H_m, H_{CH3} and H_{OCH3}, were shifted and a new pattern were appeared for ^1H NMR spectrum of porphyrin moiety of adducts.

Compound	δ N-H	δ $H_{m,p}$	δ H_o	δ H_{β}	δ OCH_3 ,CH_3
$(Me_2SnCl_2)_2H_2TPP$	0.00	7.95	8.57	8.57	-
$(Me_2SnCl_2)_2H_2T(4\text{-}Cl)PP$	0.00	8.00	8.54	8.54	-
$(Me_2SnCl_2)_2H_2T(4\text{-}CH_3)PP$	0.00	7.94	8.50	8.50	2.89
$(Me_2SnCl_2)_2H_2T(4\text{-}CH_3O)PP$	0.00	7.50	8.48	8.48	4.11
$(Et_2SnCl_2)_2H_2TPP$	0.00	8.01-04	8.56-61	8.56-61	-
$(Et_2SnCl_2)_2H_2T(4\text{-}Cl)PP$	0.06	8.09-12	8.46-55	8.46-55	-
$(Et_2SnCl_2)_2H_2T(4\text{-}CH_3)PP$	0.15	7.81-85	8.49-59	8.49-59	2.80
$(Et_2SnCl_2)_2H_2T(4\text{-}CH_3O)PP$	0.20	7.49-56	8.46-53	8.46-53	4.15
$(MeSnCl_3)_2H_2TPP$	-0.2	7.99-8.02	8.59-8.62	8.59-8.62	-
$(MeSnCl_3)_2H_2T(4\text{-}Cl)PP$	0.13	8.01-8.05	8.52-8.59	8.52-8.59	-
$(MeSnCl_3)_2H_2T(4\text{-}CH_3)PP$	0.16	7.80-7.85	8.47-8.54	8.47-8.54	2.85
$(MeSnCl_3)_2H_2T(4\text{-}CH_3O)PP$	0.22	7.55-7.58	8.53-8.55	8.53-8.55	4.16
$(Ph_2SnCl_2)_2H_2TPP$	0.00	8.05-8.07	8.64	8.64	-
$(Ph_2SnBr_2)_2H_2TPP$	-0.45	7.92-8.00	8.54-8.57	8.54-8.57	-
$(Ph_2SnCl_2)_2H_2T(4\text{-}Cl)PP$	0.00	8.04-8.07	8.53-8.62	8.53-8.62	-
$(Ph_2SnBr_2)_2H_2T(4\text{-}Cl)PP$	0.00	8.18-8.21	8.37	8.52	-
$(Ph_2SnCl_2)_2H_2T(4\text{-}CH_3)PP$	0.00	7.83-7.86	8.49-8.59	8.49-8.59	2.80
$(Ph_2SnBr_2)_2H_2T(4\text{-}CH_3)PP$	-0.30	7.83-7.86	8.51-8.56	8.51-8.56	2.79
$(Ph_2SnCl_2)_2H_2T(4\text{-}CH_3O)PP$	0.00	7.41-7.56	8.37-8.42	8.37-8.42	4.04
$(Ph_2SnBr_2)_2H_2T(4\text{-}CH_3O)PP$	0.00	7.94	8.24-8.27	8.48-8.53	4.08

Table 6. ^1H NMR chemical shift (δ/ppm) of $[(Me_2SnCl_2)_2H_2T(4\text{-}X)PP]$ adducts relative to $CHCl_3$.

Comparing the chemical shifts of different protons of the free base $H_2T(4\text{-}X)PPs$ with the same protons of $H_2T(4\text{-}X)PPs$ in its complexes some useful information can be induced. The internal N-H signal moves downfield (≈2.7-2.8 ppm) and H_β protons signal move upfield (≈0.25-0.31 ppm). Both changes are discontinuous and are in the directions to be expected if the aromatic ring current decreases with the interaction of free base porphyrins with organotin(IV) halides. The two aromatic proton doublets related to the H_o and $H_{m,p}$ of the phenyl rings in H_2TPP, also H_o and H_m of phenyl of the $H_2T(4\text{-}X)PPs$, moves downfield (≈0.31-0.25 ppm) and $H_{CH3}(H_{OCH3})$ singlets of $H_2T(4\text{-}X)PPs$ (X= CH_3 and CH_3O) moves downfield (≈0.31-0.14 ppm). These changes can be described by decreasing the aromatic ring current because of the coordination of porphyrin to the organotin(IV) halide Lewis acids that led to deformation of porphyrin structure from planarity. Such changes were seen in the SAT complexes, let alone the paramagnetic property of Cu(II) ion which lead to some differences between ^1H NMR spectra of SAT complexes with our adducts. Also the ^1H NMR spectra of these adducts are comparable with related porphyrin dication.[25-27] Concerning the ^1H NMR spectra of 22,24-dihydro-5,10,15,20-tetraphenylporphyrin diperchlorate $[H_4TPP^{2+}][ClO_4^-]_2$; N-H (-2.47 ppm), $H_{m,p}$(8.04 ppm), H_o (8.61), H_β (8.77ppm) and 22,24-dihydro-5,10,15,20-tetraphenylporphyrin dihydrogen sulfate $[H_4TPP^{2+}][HSO_4^-]_2$; N-H (-1.21 ppm), $H_{m,p}$(7.82 ppm), H_o (8.45), H_β (8.51ppm) , (δ relative to TMS in $CDCl_3$) similar trends can be found between ^1H NMR chmical shift of porphyrin dication and our adducts.

According to ^1H NMR pattern these adducts have symmetrical structures, so that coordination to organotin(IV) halides couldn't differ between each class of free base porphyrin protons (N-H, H_β, H_o, and …) upon adduct formation and these protons remained equivalent after complex formation. Referring to elemental analysis data these adducts have the mole ratio 2:1 of acceptor to donor, $[(R_2SnCl_2)_2(H_2T(4\text{-}X)PP)]$.

In Fig. 6 (a), because of attachment of tin atoms to two pyrrolenine nitrogens, splitting of ^1H NMR signal of pyrroles and pyrrolenine Hβs and producing a doublet band for beta hydrogens is expected, a singlet for pyrroles Hβs and a singlet for pyrrolenines Hβs. On the other hand, in Fig. 6 (b) and (c) Hβs have relatively identical environment, therefore we predict a singlet band for both pyrroles and pyrrolenine Hβs, but in Fig. 6 (c) because of high steric congestion of N-H pyrrole hydrogens with organotin(IV) halide upon adduct formation, doesn't seem it has a significant apart in adduct structure. Experimentally, in the low-temperature ^1H NMR spectra of adducts a singlet was appeared for Hβs, referring to S. Funahashi results on slowness of the N-H tautomerism in the SAT complex with respect to the time scale of the ^1H NMR at 21 °C,[16] it is confirming the Fig. 6 (b) structure for these adducts. On the basis of these results we suggest that free base porphyrin as a bidentate bridging ligand make a bridge between two molecules of the Lewis acid through it's nitrogenes lone pairs. It is probable that two neighbor nitrogen atoms (a pyrrole and a pyrrolenine nitrogen) of the porphyrin binded to one of the R_2SnCl_2 molecules which posited on the above of the porphyrin plane and the other two nitrogen atoms (a pyrrole and a pyrrolenine nitrogen) binded to the second R_2SnCl_2 molecule from below of this plane. Therefore we have a structure close to that suggested by K.M. Smith et al. for XHg-TPP-HgX, X= Cl^- and CH_3COO^-.[29]

Interactions of organotin(IV) halides with free base $H_2T(4\text{-}X)PP$ are very sensitive to temperature and donor property of the solvent, *Fig.* 7. By increasing the temperature the

green color of the adduct solution changes to brown and the color return to the primary color of free base porphyrin solution, eventually. Also these adduct formations were not observed in ligating solvents such as CH_3CN and DMSO under these conditions.

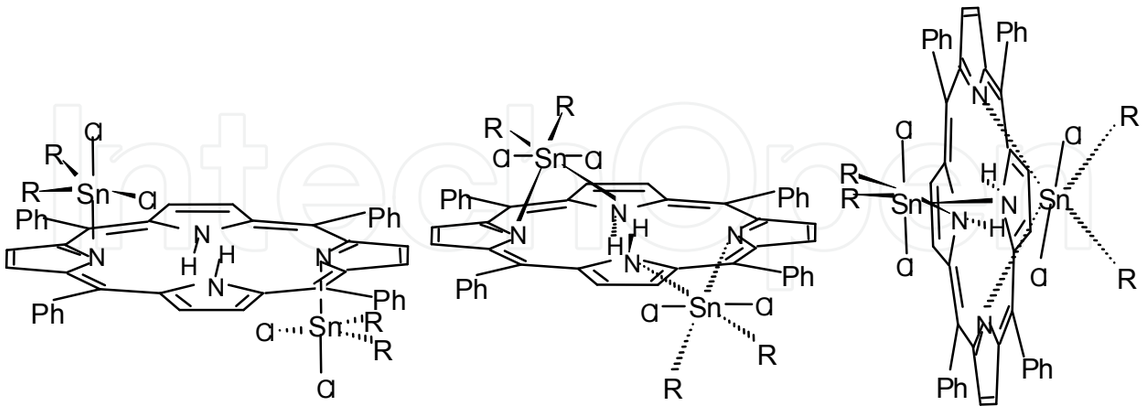

(a) (b) (c)

Fig. 6. Proposed structures of $[(R_2SnCl_2)_2H_2TPP]$ adducts. (a) H_2TPP as a monodentate bridging ligand made adducts with five-coordinated trigonal bipyramidal structure for tin atoms; (b) and (c) H_2TPP as a bidentate bridging ligand make adducts with six-coordinated octahedral structure around the tin atoms. Our ^1H NMR data are in consistent with structure (b).

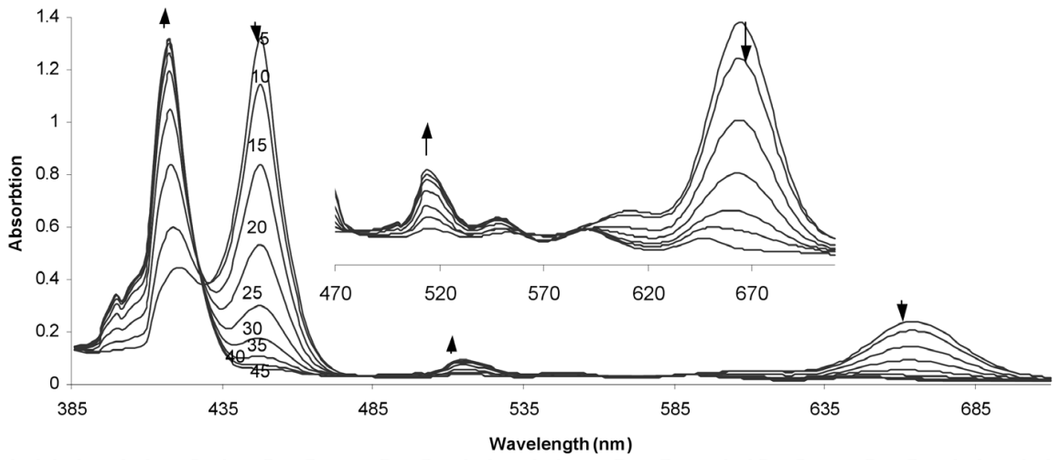

Fig. 7. The temperature dependence change of the absorption profile of the $[(Me_2SnCl_2)_2H_2T(4\text{-}Cl)PP]$ adduct in chloroform: By addition of Me_2SnCl_2 (0.0125 M, 0.5 ml) to the solution of $H_2T(4\text{-}Cl)PP$ (5×10^{-6} M, 2.5 ml) in chloroform in an UV-vis cell at 5 °C, the $(Me_2SnCl_2)_2H_2T(4\text{-}Cl)PP$ adduct was formed. Then the composition of the cell was remained constant and the temperature was raised to 45 °C, stepwisely.

1.4.2.2 Basicity of the free base porphyrins:

The basicity of the free base porphyrins toward proton is usually determined when possible by pK_3 measurements for the dissociation of the mono-cation $H_3T(4\text{-}X)PP^+$ into the free base $H_2T(4\text{-}X)PP$ measured in detergent solutions:

$$H_3T(4\text{-}X)PP^+ = H_2T(4\text{-}X)PP + H^+ \quad K_3 \tag{9}$$

On the other hand, the basicity of the porphyrins have been related to the reduction potential (in volts) of the free base porphyrin to its radical anion form.[30] The value of $E_{1/2}(1)$ for some of the free base porphyrins in DMF is given in Table 7.

$$H_2T(4\text{-}X)PP + e \rightleftharpoons H_2T(4\text{-}X)PP^- \quad E_{1/2}(1) \tag{10}$$

X	NO_2	Cl	H	CH_3	CH_3O
$E_{1/2}(1)$	-1.34	-1.47	-1.55	-1.57	-1.59

Table 7. Reduction potentials (in volts) for $H_2T(4\text{-}X)PPs$ (in DMF, 25 °C).[30]

A linear relationship between pK_3 and $E_{1/2}(1)$ has been reported for some of porphyrins:

$$pK_3 = -5.9\ E_{1/2}(1) - 5.2$$

according to this Equation the most basic porphyrins are the more difficult to reduce. Therefore, more negative values of $E_{1/2}(1)$ are indicating stronger basic properties of free base porphyrin.

1.4.2.3 The thermodynamic studies

The thermodynamic parameters are useful tools for studying the interactions between the donor and the acceptor molecules. The first step in these studies is the determination of formation constants, which make help to better understanding of relative stability of molecular adducts. In these studies we used the SQUAD program [31] for data refinement. This program is designed to calculate the best values for the equilibrium constants of the proposed equilibrium model by employing a non-linear least-squares approach and UV-vis data. The formation constants and thermodynamic parameters ΔH^o, ΔS^o and ΔG^o values for different systems are listed in Tables 8 and 9, respectively.

According to results presented for molecular interactions of organotin(IV) halides with free base porphyrins the following order was obtained for acceptor properties of organotin(IV) Lewis acids:

$$MeSnBr_3 > Me_2SnCl_2 > Ph_2SnCl_2 > Ph_2SnBr_2 > Et_2SnCl_2 > Bu_2SnCl_2$$

This trend shows that interaction of organotin(IV) halides with free base porphyrins become weaker by increasing the electron-releasing and the steric hindrance of substituents on the tin atom.

On the other hand, results show the effect of X substituents of phenyl rings of free base porphyrins on the stability of adducts, explicitly. Considering data given in Tables 8 and 9 for the interaction of organotin(IV) Lewis acids with free base porpyrins, $H_2T(4\text{-}X)PP$ (X= H, Cl, CH_3, CH_3O, NO_2), basicity of free base porphyrins for interaction with organotin(IV) halides decreases as follows:

$$H_2T(4\text{-}CH_3O)PP > H_2T(4\text{-}CH_3)PP > H_2TPP > H_2T(4\text{-}Cl)PP > H_2T(4\text{-}NO_2)PP$$

Of course, $H_2T(4\text{-}NO_2)PP$ under our working conditions (concentration and temperature) did not show a measurable interaction with diorganotin(IV) dihalides.

Adduct	lgK				
	5 °C	10 °C	15 °C	20 °C	25 °C
$[(Me_2SnCl_2)_2H_2TPP]$	7.61± 0.02	6.95± 0.01	6.46± 0.01	5.81± 0.01	5.05± 0.01
$[(Me_2SnCl_2)_2H_2T(4\text{-}Cl)PP]$	6.10± 0.01	5.66± 0.01	5.14± 0.01	4.64± 0.01	-
$[(Me_2SnCl_2)_2H_2T(4\text{-}CH_3)PP]$	10.06±0.01	9.30± 0.01	8.46± 0.01	7.81± 0.01	6.99± 0.01
$[(Me_2SnCl_2)_2H_2T(4\text{-}CH_3O)PP]$	10.25± 0.01	9.43± 0.01	8.69± 0.01	7.96± 0.01	7.20± 0.01
$[(Et_2SnCl_2)_2H_2TPP]$	6.38 ± 0.02	5.87 ± 0.01	5.53 ± 0.02	5.08 ± 0.04	-
$[(Et_2SnCl_2)_2H_2T(4\text{-}Cl)PP]$	5.25 ± 0.02	4.76 ± 0.01	4.36 ± 0.02	4.04 ± 0.04	
$[(Et_2SnCl_2)_2H_2T(4\text{-}CH_3)PP]$	6.96 ± 0.01	6.51 ± 0.01	6.04 ± 0.04	5.45 ± 0.05	5.11 ± 0.02
$[(Et_2SnCl_2)_2H_2T(4\text{-}CH_3O)PP]$	8.08 ± 0.03	7.34 ± 0.02	7.04 ± 0.04	6.38 ± 0.02	5.93 ± 0.01
$[(Bu_2SnCl_2)_2H_2TPP]$	5.69 ± 0.01	5.34 ± 0.02	4.88 ± 0.01	4.38 ± 0.02	4.04 ± 0.04
$[(Bu_2SnCl_2)_2H_2T(4\text{-}Cl)PP]$	4.70 ± 0.01	4.32 ± 0.02	3.82 ± 0.01	3.54 ± 0.01	3.11 ± 0.02
$[(Bu_2SnCl_2)_2H_2T(4\text{-}CH_3)PP]$	6.89 ± 0.01	6.40 ± 0.02	5.99 ± 0.01	5.32 ± 0.02	5.15 ± 0.02
$[(Bu_2SnCl_2)_2H_2T(4\text{-}CH_3O)PP]$	7.85 ± 0.01	7.15 ± 0.02	6.76 ± 0.01	6.20 ± 0.02	5.80 ± 0.01
$(Ph_2SnCl_2)_2H_2TPP$	7.12±0.01	6.46±0.01	5.57±0.09	5.25±0.04	4.24±0.01
$(Ph_2SnCl_2)_2H_2T(4\text{-}Cl)PP$	6.32±0.02	5.90±0.03	5.40±0.09	4.85±0.04	4.10±0.01
$(Ph_2SnCl_2)_2H_2T(4\text{-}CH_3)PP$	8.02±0.01	7.66±0.01	6.69±0.09	5.94±0.03	5.10±0.02
$(Ph_2SnCl_2)_2H_2T(4\text{-}CH_3O)PP$	9.90±0.02	9.04±0.02	8.20±0.09	7.50±0.02	6.63±0.04
$(Ph_2SnBr_2)_2H_2TPP$	6.45±0.01	6.00±0.02	5.36±0.09	4.83±0.07	4.07±0.08
$(Ph_2SnBr_2)_2H_2T(4\text{-}Cl)PP$	5.91±0.01	5.33±0.01	5.07±0.09	4.71±0.09	4.05±0.08
$(Ph_2SnBr_2)_2H_2T(4\text{-}CH_3)PP$	7.50±0.02	6.80±0.02	5.71±0.09	5.35±0.06	4.81±0.05
$(Ph_2SnBr_2)_2H_2T(4\text{-}CH_3O)PP$	9.20±0.02	8.40±0.02	7.52±0.09	6.68±0.06	6.13±0.05
$(MeSnBr_3)_2H_2TPP$	12.51 ± 0.06	11.33± 0.03	10.46± 0.03	9.58 ± 0.03	8.45 ± 0.02
$(MeSnBr_3)_2H_2T(4\text{-}Cl)PP$	11.41 ± 0.03	10.56± 0.04	9.75 ± 0.02	9.15 ± 0.02	7.95 ± 0.02
$(MeSnBr_3)_2H_2T(4\text{-}NO_2)PP$	6.68 ± 0.01	6.11 ± 0.03	5.58 ± 0.05	4.90 ± 0.08	4.41 ± 0.04
$(MeSnBr_3)_2H_2T(4\text{-}CH_3)PP$	13.61 ± 0.06	12.49± 0.06	11.53± 0.04	10.45± 0.04	9.31 ± 0.05
$(MeSnBr_3)_2H_2T(4\text{-}CH_3O)PP$	14.28 ± 0.03	13.12± 0.03	11.96± 0.02	10.88± 0.02	9.76 ± 0.09

Table 8. The formation constants lgK for $H_2T(4\text{-}X)PP$ adducts in $CHCl_3$ solvent.

Adducts have negative values of ΔH^{o}, ΔS^{o}, and ΔG^{o} (Table 9) which correspond to exothermic adduct formations between organotin(IV) Lewis acids and free base porphyrins.

Adduct	$-\Delta H^{o}$	$-\Delta S^{o}$	$-\Delta G^{o}$ [b]
$(Me_2SnCl_2)_2H_2TPP$	199 ±11	569 ± 33	38 ±11
$(Me_2SnCl_2)_2H_2T(4\text{-}Cl)PP$	167 ± 7	483 ± 25	30 ±7
$(Me_2SnCl_2)_2H_2T(4\text{-}CH_3)PP$	242 ± 7	678 ± 26	50 ± 7
$(Me_2SnCl_2)_2H_2T(4\text{-}CH_3O)PP$	240 ± 8	668 ± 31	51 ± 8
$(Et_2SnCl_2)_2H_2TPP$	138 ± 5	373 ± 19	32 ± 5
$(Et_2SnCl_2)_2H_2T(4\text{-}Cl)PP$	128 ± 8	360 ± 28	26 ± 8
$(Et_2SnCl_2)_2H_2T(4\text{-}CH_3)PP$	150 ± 6	405 ± 23	35 ± 6
$(Et_2SnCl_2)_2H_2T(4\text{-}CH_3O)PP$	168 ± 10	451 ± 35	40 ± 10
$(Bu_2SnCl_2)_2H_2TPP$	136 ± 5	378 ± 19	29 ± 5
$(Bu_2SnCl_2)_2H_2T(4\text{-}Cl)PP$	124 ± 5	356 ± 18	23 ± 5
$(Bu_2SnCl_2)_2H_2T(4\text{-}CH_3)PP$	142 ± 7	379 ± 26	35 ± 7
$(Bu_2SnCl_2)_2H_2T(4\text{-}CH_3O)PP$	160 ± 7	427 ± 25	39 ± 7
$(Ph_2SnCl_2)_2H_2TPP$	216 ±17	644 ±58	34 ±17
$(Ph_2SnCl_2)_2H_2T(4\text{-}Cl)PP$	174 ±11	508 ±40	31 ±11
$(Ph_2SnCl_2)_2H_2T(4\text{-}CH_3)PP$	234 ±18	688 ±58	39 ±18
$(Ph_2SnCl_2)_2H_2T(4\text{-}CH_3O)PP$	251 ±5	717 ±16	48 ±5
$(Ph_2SnBr_2)_2H_2TPP$	184 ±11	538 ±37	32 ±11
$(Ph_2SnBr_2)_2H_2T(4\text{-}Cl)PP$	138 ±12	382 ±44	29 ±12
$(Ph_2SnBr_2)_2H_2T(4\text{-}CH_3)PP$	213 ±20	625 ±70	36 ±20
$(Ph_2SnBr_2)_2H_2T(4\text{-}CH_3O)PP$	244 ±8	707 ±30	44 ±5
$(MeSnBr_3)_2H_2TPP$	301 ±11	845 ±37	61 ±11
$(MeSnBr_3)_2H_2T(4\text{-}Cl)PP$	264 ±17	730 ±60	57 ±17
$(MeSnBr_3)_2H_2T(4\text{-}NO_2)PP$	182 ±5	528 ±17	32 ±5
$(MeSnBr_3)_2H_2T(4\text{-}CH_3)PP$	337 ±8	953 ±28	67 ±8
$(MeSnBr_3)_2H_2T(4\text{-}CH_3O)PP$	358 ±2	1014 ±8	71 ±2

[a] ΔH^{o} (kJ.mol^{-1}), ΔS^{o} (J.K^{-1}. mol^{-1}), and ΔG^{o} at 10 °C (kJ. mol^{-1}).

Table 9. The thermodynamic parameters ΔH^{o}, ΔS^{o} and ΔG^{o} for $H_2T(4\text{-}X)PP$ adducts in $CHCl_3$.[a]

2. Molecular interactions of organic π-acceptors with $H_2T(4\text{-}X)PP$ (X= H, Cl, CH_3, CH_3O)

Intermolecular charge-transfer **(CT)** complexes are formed when electron donors and electron acceptors interact, a general phenomenon in organic chemistry. Mulliken [32] considered such complexes to arise from a Lewis acid-Lewis base type of interaction, the bond between the components of the complex being postulated to arise from the partial transfer of an π electron from the base to orbitals of the acid. TCNE, DDQ, TBBQ and TCBQ can form **CT** complexes when mixed with molecules possessing π-electrons or groups having atoms with an unshared electron pair [33-35]. The thermodynamic of CT complexes of several free base tetraaryl- as well as tetraalkylporphyrins with organic π-acceptors TCNE, DDQ, TBBQ and TCBQ have been investigated. It would be instructive to compare their thermodynamic parameters since it improve our insight about characteristics of their interactions and efficiency of their applications.

Adducts which have been prepared from mixing of organic π-acceptors with a solution of free base porphyrin in dry chloroform, those ^{1}H NMR and UV-vis data were been given in Tables 10-12.

Compound	δN-H	$\delta H_{m,p}$	δH_o	δH_β	δCH_3
H_2TPP	-2.76	7.75	8.24	8.85	-
$(TCNE)_2H_2TPP$	-1.26	8.04	8.64	8.81	-
$(DDQ)_2H_2TPP$	-0.40	7.98	8.67	8.59	-
$(TCBQ)_2H_2TPP$	-2.00	7.79	8.28	8.81	
$(TBBQ)_2H_2TPP$	-0.13	8.06	8.67	8.81	
$H_2T(4\text{-}Cl)PP$	-2.86	7.75	8.14	8.85	-
$(TCNE)_2H_2T(4\text{-}Cl)PP$	-1.16	8.05	8.57	8.81	-
$(DDQ)_2H_2T(4\text{-}Cl)PP$	-0.29	8.00	8.56	8.56	-
$(TCBQ)_2H_2T(4\text{-}Cl)PP$	-2.60	7.76	8.20	8.83	
$(TBBQ)_2H_2T(4\text{-}Cl)PP$	-0.11	7.80	8.58	8.83	
$H_2T(4\text{-}CH_3)PP$	-2.77	7.56	8.11	8.86	2.71
$(TCNE)_2H_2T(4\text{-}CH_3)PP$	-1.20	7.83	8.52	8.76	2.80
$(DDQ)_2H_2T(4\text{-}CH_3)PP$	-0.38	7.80	8.55	8.55	2.77
$(TCBQ)_2H_2T(4\text{-}CH_3)PP$	-2.10	7.57	8.12	8.84	2.75
$(TBBQ)_2H_2T(4\text{-}CH_3)$	-0.73	7.57	8.12	8.84	2.75
PP $H_2T(4\text{-}CH_3O)PP$	-2.82	7.27	8.11	8.86	3.95
$(TCNE)_2H_2T(4\text{-}OCH_3)PP$	-0.92	7.55	8.57	8.68	4.17
$(DDQ)_2H_2T(4\text{-}OCH_3)PP$	-0.11	7.50	8.59	8.48	4.11
$(TCBQ)_2H_2T(4\text{-}OCH_3)PP$	-1.16	7.27	8.13	8.76	3.96
$(TBBQ)_2H_2T(4\text{-}OCH_3)PP$	-0.12	7.60	8.40	8.76	4.10

Table 10. ^{1}H NMR of free base tetraarylporphyrins and their adduct with DDQ and TCNE.

The schematic chemical equilibria for interaction of molecular π-acceptors with free base porphyrins could be written according to Equation 11: [36-38]

$$2(\pi\text{-acceptor}) + (\text{free base porphyrin}) \leftrightarrow (\pi\text{-acceptor})_2(\text{free base porphyrin}) \quad (11)$$

2.1 ^{1}H NMR analysis

^{1}H NMR analysis: in the ^{1}H NMR spectra of adducts the signals correspond to N-H, H_o, $H_{m,p}$, and CH_3- or -OCH_3 protons of tetraarylporphyrin moved downfield, while H_β has an upfield shift (Table 11). But tetraalkylporphyrins, the signals correspond to H_β has an upfield shift the N-H signal in 5 and 11 moved downfield while for 6 and 12 upfield shift observed for this proton with adduct formation (Table 12).

Compound	δN-H	δCH_3	δCH_2	δCH_2	δCH_2	δH_β
H_2TnBP	-2.61	1.10	1.73-1.91	2.41-2.58	4.88	9.45
$(TCNE)_2H_2TnBP$	-3.45	1.22	1.93	2.54	4.83	9.03
$(DDQ)_2H_2TnPP$	-3.45	1.20	1.90	2.55	4.81	9.02
H_2TtBP	1.52	2.01	-	-	-	9.08
$(TCNE)_2H_2TtBP$	-0.4	2.13	-	-	-	8.14
$(DDQ)_2H_2TtBP$	-0.6	2.10	-	-	-	8.16

Table 11. ^{1}H NMR of free base tetraalkylporphyrins and their adduct with DDQ and TCNE.

2.2 Infra red spectra

The most significant difference which emerges from a comparison of the vibrational spectra of free base porphyrins and their molecular adducts with π-acceptor molecules is disappearance of the band ν(N–H) as a consequence of the complex formation. It seams that N–H was contributed in intermolecular hydrogen bonds that formed between its proton and N or O atoms of π-acceptor molecules. The IR spectra of free TCNE shows CN stretching frequencies at 2225 and 2270 cm^{-1}. The significant shift of these CN vibrations toward lower frequencies (2214 cm^{-1}) is indicating charge transferring from free base porphyrins to an π^* orbital of CN group of TCNE. This charge transfer phenomenon leads to weakening of corresponding C≡N bond. Similarly, in the free DDQ the CO and the CN stretching frequencies were appeared at 1675 and 2245 cm^{-1}, respectively. Upon complex formation the CO vibrations shift to 1651 and 1696 cm^{-1} and CN vibration shift to 2229 cm^{-1}.

Compound	λ/nm	Compound	λ/nm
$(TCNE)_2H_2TPP$	441 653	$(TCNE)_2H_2T(4\text{-}OCH_3)PP$	454 653
$(DDQ)_2H_2TPP$	445 663	$(DDQ)_2H_2T(4\text{-}OCH_3)PP$	453 688
$(TCBQ)_2H_2TPP$	445 662	$(TCBQ)_2H_2T(4\text{-}OCH_3)PP$	443 688
$(TBBQ)_2H_2TPP$	447 666	$(TBBQ)_2H_2T(4\text{-}OCH_3)PP$	445 694
$(TCNE)_2H_2T(4\text{-}Cl)PP$	443 652	H_2TnBP	417 520 555 600 659
$(DDQ)_2H_2T(4\text{-}Cl)PP$	448 652	$(TCNE)_2H_2TnBP$	425 636
$(TCBQ)_2H_2T(4\text{-}Cl)PP$	447 665	$(DDQ)_2H_2TnPP$	433 643
$(TBBQ)_2H_2T(4\text{-}Cl)PP$	450 669	H_2TtBP	448 552 596 628 691
$(TCNE)_2H_2T(4\text{-}CH_3)PP$	445 653	$(TCNE)_2H_2TtBP$	451 690
$(DDQ)_2H_2T(4\text{-}CH_3)PP$	447 677	$(DDQ)_2H_2TtBP$	455 692
$(TCBQ)_2H_2T(4\text{-}CH_3)PP$	448 672		
$(TBBQ)_2H_2T(4\text{-}CH_3)PP$	450 678		

Table 12. UV-vis peaks (λ/nm in $CHCl_3$) of FBPs and $[(A)_2D]$ adducts.

2.3 UV-vis analysis

By interaction of free base porphyrin with π-acceptor molecules, their original peaks changed to a new pattern with two new peaks which their positions show about 20-40 nm red shift relative to the band V (Soret band) and the band I (of Q band) of free base $H_2T(4\text{-}X)PPs$, Table 10.

π-Acceptor molecules show different behaviors in their interactions with free base porphyrins. For DDQ the interactions were found exothermic and stability of adducts decreased at elevated temperatures, so that a solution of adduct at 5 °C goes to a solution containing dissociated free base and DDQ molecules when temperature were raised to 35 °C. It shows that by increasing of temperature the corresponding equilibrium in Equation 11 is shifted to the left.

On the other hand, for TCNE, TBBQ and TCBQ interactions are endothermic and at elevated temperatures the stability of adducts increased, so that a purple solution of reactant at 5 °C turns to a green solution of adduct at 35 °C. It means that, for these acceptors the equilibrium in Equation 11 is going to completion at higher temperatures.

2.4 Thermodynamic studies

The thermodynamic parameters were investigated for these interactions by UV-vis spectrometry method. The formation constants, K, were determined at several temperatures by analyzing the concentration and temperature dependence of UV-vis absorptions using the SQUAD program, Tables 13 and 14. Van't Hoff plots of these formation constants were used for obtaining the other thermodynamic parameters $\Delta H°$, $\Delta S°$, and $\Delta G°$ (Table 15).

The data of Table 13 shows that stability of adducts for all acceptors undergo a regular increase from $H_2T(4\text{-Cl})PP$ to H_2TPP, $H_2T(4\text{-}CH_3)PP$, and $H_2T(4\text{-}OCH_3)PP$; also adducts of H_2TtBP are more stable than H_2TnBP. These sequences are in agreement with electron releasing property of free base porphyrins.

Adduct	lg K				
	5 °C	10 °C	15 °C	20 °C	25 °C
$(TCNE)_2H_2TPP$	5.72±0.02	6.47±0.02	6.79±0.01	7.33±0.03	8.03±0.02
$(TCNE)_2H_2T(4\text{-Cl})PP$	4.40±0.01	5.01±0.02	5.42±0.01	6.20±0.03	6.45±0.02
$(TCNE)_2H_2T(4\text{-}CH_3)PP$	6.10±0.02	6.65±0.03	7.06±0.01	7.88±0.02	8.36±0.01
$(TCNE)_2H_2T(4\text{-}OCH_3)PP$	6.30±0.02	6.87±0.03	7.30±0.01	8.00±0.03	8.62±0.01
$(TCNE)_2H_2TnBP$	6.03±0.02	6.33±0.03	6.82±0.01	7.06±0.03	7.30±0.01
$(TCNE)_2H_2TtBP$	7.51±0.02	7.86±0.03	8.29±0.01	8.59±0.02	8.80±0.01
$(DDQ)_2H_2TPP$	9.66±0.02	9.41±0.01	9.24±0.01	9.06±0.03	8.83±0.01
$(DDQ)_2H_2T(4\text{-Cl})PP$	9.50±0.01	9.24±0.02	9.09±0.03	8.92±0.01	8.70±0.02
$(DDQ)_2H_2T(4\text{-}CH_3)PP$	10.11±0.01	9.85±0.01	9.64±0.03	9.45±0.01	9.24±0.02
$(DDQ)_2H_2T(4\text{-}OCH_3)PP$	10.34±0.02	10.12±0.02	9.93±0.04	9.69±0.01	9.42±0.03
$(DDQ)_2H_2TnPP$	9.45±0.02	9.30±0.02	9.13±0.04	8.95±0.01	8.81±0.03
$(DDQ)_2H_2TtBP$	10.17±0.02	10.01±0.02	9.81±0.04	9.62±0.01	9.48±0.03

Table 13. The formation constants lgK for $H_2T(4\text{-X})PP$ adducts in $CHCl_3$ solvent.

Adduct	lg K				
	15 °C	20 °C	25 °C	30 °C	35 °C
$(TCBQ)_2H_2T(4\text{-Cl})PP$	3.89±0.03	4.17±0.09	4.51±0.08	4.70±0.07	5.00±0.09
$(TCBQ)_2H_2TPP$	4.07±0.06	4.39±0.06	4.64±0.07	4.98±0.09	5.20±0.06
$(TCBQ)_2H_2T(4\text{-}CH_3)PP$	4.41±0.09	4.80±0.09	5.01±0.04	5.32±0.09	5.58±0.04
$(TCBQ)_2H_2T(4\text{-}OCH_3)PP$	4.97±0.04	5.35±0.04	5.70±0.08	6.05±0.03	6.34±0.03
$(TBBQ)_2H_2T(4\text{-Cl})PP$	5.66±0.06	6.01±0.09	6.42±0.08	6.67±0.08	7.00±0.09
$(TBBQ)_2H_2TPP$	6.70±0.06	7.20±0.06	7.69±0.09	8.20±0.08	8.50±0.08
$(TBBQ)_2H_2T(4\text{-}CH_3)PP$	6.86±0.07	7.45±0.07	7.85±0.08	8.67±0.09	9.00±0.08
$(TBBQ)_2H_2T(4\text{-}OCH_3)PP$	7.00±0.07	751±0.05	7.93±0.07	8.93±0.07	9.18±0.08

Table 14. The formation constants lgK for $H_2T(4\text{-X})PP$ adducts in $CHCl_3$ solvent.

Table 13 shows that formation constants for interaction of DDQ with free base porphyrins decreased at higher temperatures. In contrast for other acceptors (TCNE, TBBQ and TCBQ)

formation constants increased at higher temperatures. This discrepancy might be due to presence of different mechanisms for caring out charge transfer between free bases and these π-acceptors. Since these π-acceptors are common oxidizing agents in organic chemistry, this dual influence of temperatures on their interactions with free base porphyrins is an interesting point that less has been attended previously. According to formation constants the following order was suggested for acceptor property of these molecules: DDQ ⟩TCNE ⟩ TBBQ ⟩ TCBQ

Table 15 gives the thermodynamic parameters (ΔH°, ΔS°, and ΔG°) for charge transfer adducts of DDQ, TCNE, TBBQ and TCBQ with free base porphyrins in chloroform. These results show that meso-group of free base porphyrins significantly affected strength of their interactions with acceptor species. While electron releasing meso-groups improves interactions of free base porphyrins with π-acceptors molecules, electron withdrawing meso-groups diminished these interactions.

Compound	Δ*H*°	Δ*S*°	-Δ*G*°	Compound	Δ*H*°	Δ*S*°	-Δ*G*°
$(TCNE)_2H_2TPP$	174±12	734±43	45±12	$(TCBQ)_2H_2T(4\text{-}CH_3)PP$	101±6	435±19	29±1
$(DDQ)_2H_2TPP$	-64±3	-45±10	50±3	$(TBBQ)_2H_2T(4\text{-}CH_3)PP$	168±14	714±45	45±1
$(TCBQ)_2H_2TPP$	98±7	416±23	27±1	$(TCNE)_2H_2T$	183±10	784±33	51±10
$(TBBQ)_2H_2TPP$	160±6	683±23	44±12	$(4\text{-}OCH_3)$ PP			
$(TCNE)_2H_2T(4\text{-Cl})PP$	168±12	688±43	37±12	$(DDQ)_2H_2T$	-72±4	-61±12	54±4
$(DDQ)_2H_2T(4\text{-Cl})PP$	-61±3	-38±10	49±3	$(4\text{-}OCH_3)$ PP			
$(TCBQ)_2H_2T(4\text{-Cl})PP$	94±5	401±18	26±1	$(TCBQ)_2H_2T$	109±3	509±9	33±1
$(TBBQ)_2H_2T(4\text{-Cl})PP$	116±5	512±15	36±1	$(4\text{-}OCH_3)$ PP			
$(TCNE)_2H_2T$	179±10	761±35	47±10	$(TBBQ)_2H_2T$	197±37	816±124	46±1
$(4\text{-}CH_3)PP$				$(4\text{-}OCH_3)$ PP			
$(DDQ)_2H_2T$	-68±2	-52±7	52±3	$(TCNE)_2H_2TnBP$	107±7	495±26	40±7
$(4\text{-}CH_3)PP$				$(DDQ)_2H_2TnPP$	-53±1	38±4	41±1
				$(TCNE)_2H_2TtBP$	109±6	529±22	49±6
				$(DDQ)_2H_2TtBP$	-63±3	-26±11	70±3

[a] Δ*H*°(kJ mol^{-1}) and Δ*S*° (J K^{-1} mol^{-1}); Δ*G*° at 25 °C (kJ mol^{-1}).

Table 15. The thermodynamic parameters for [$(Acceptor)_2$(Free base porphyrin)] adducts in $CHCl_3$.[a]

For $[(DDQ)_2FBP]$ adducts, Δ*H*° and Δ*S*° are negative. But other adducts ($[(TCNE)_2FBP]$, $[(TBBQ)_2FBP]$, $[(TCBQ)_2FBP]$) have positive values for Δ*H*° and Δ*S*° parameters. Since interactions of free base porphyrins with various acceptors are exothermic, endothermic interactions for these π-acceptors are interesting and unexpected. It seems presence of strong self π-stacking between these π-acceptor molecules make their dissolving endothermic, on the other hand dissociation of such π-stacks make their dissolving, entropically a favorable phenomena.

The standard Gibbs free energies, Δ*G*°, of interactions are negative in all cases. It seems that for TCNE, TBBQ and TCBQ term $\Delta S^o \rangle 0$ is more effective than $\Delta H^o \rangle 0$ in the following Equation: Δ*G*° = Δ*H*° - TΔ*S*° so that negative values for Δ*G*° were occurred. Negative values

of $\Delta G°$ show that interactions of these molecules with free bases are favorable with the same ordering as their electron releasing property.

The main goal in this work is "positive $\Delta H°$" for TCNE, TBBQ and TCBQ adducts. In view of the discrepancy, further studies are certainly necessary to clarify this essential issue. Our results are indicating that electron acceptor properties of these molecules depend on temperature and this might be important to consider it for facilitating their subsequent applications.

3. Hydrogen bond complexes of 2,4-dichloro-; 2,4,6-trichloro- and 4-nitrophenol with free bases *meso*-tetraarylporphyrins

Hydrogen bonds play a crucial role in many chemical, physical, and biochemical processes, and they are also very important in crystal engineering [39-42]. Hydrogen bonds usually designated as X-H…Y in which there is an X-H proton donating bond and an acceptor of protons (Y-center). Interaction of phenol derivatives (PD) such as 4-nitrophenol (4NP), 2,4-Dichlorophenol (24DCP), and 2,4,6-Trichlorophenol (246)TCP with biological systems are of interest. Porphyrins with two N-H proton donating sites and numerous nitrogen atoms as proton acceptor centers can form HB complexes with some hydroxylated compounds. Last studies were demonstrated that hydrogen bonded complexes of phenol derivatives with free base porphyrins has a 2:1 mole ratio of phenol to porphyrin.

On addition of phenol derivatives (PD; 4NP, 24DCP and 246TCP) to a solution of $H_2T(4\text{-}X)PP$ in chloroform, PD form HB complex with free base porphyrin according to following equation: [43, 44]

$$2PD + H_2T(4\text{-}X)PP \rightleftharpoons (PD)2H_2T(4\text{-}X)PP \tag{12}$$

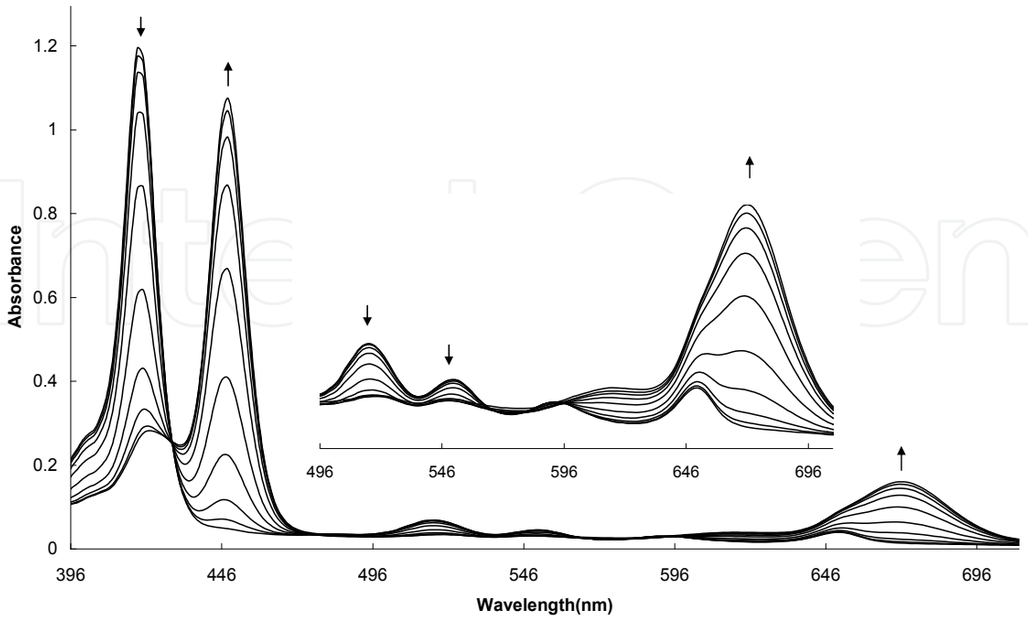

Fig. 8. Titration spectra for interaction of 24DCP with $H_2T(4\text{-}CH_3O)PP$ in chloroform. Bands appeared at 455 and 688 nm are related to adduct, isosbestic point at 428.

These interactions were studied by means of UV-vis spectrometry method and data refinement were carried out by SQUAD program. Interaction of PDs with free base porphyrins leads to a fundamental change in the porphyrins electronic absorption spectra, Fig.8 and Table 16. For example, when a solution of $H_2T(4\text{-}CH_3O)PP$ in chloroform was interacted with 24*DCP*, the original peaks of $H_2T(4\text{-}CH_3O)PP$ were vanished and adduct peaks' were appeared at 455 and 688 nm. A clear isosbestic point at 428 nm represents formation of hydrogen bond complex in a reversible reaction. For experimental illustration of an endothermic equilibrium adduct formation a solution of $[(PD)_2H_2T(4\text{-}CH_3)PP]$ adduct at 25 °C was cooled to 5 °C in a UV-vis cell. Observations show that upon cooling the adduct $[(PD)_2H_2T(4\text{-}CH_3)PP]$ with Soret band at 445 nm was dissociated to PD and free base porphyrin $H_2T(4\text{-}CH_3)PP$ with Soret band at 419 nm. By heating of solution to 25 °C the adduct was formed again and Soret band was returned to 445 nm (Fig. 9).

Compound	λ (nm)		Compound	λ (nm)	
$(24DCP)_2H_2TPP$	445	651	$(246TCP)_2H_2T(4\text{-}CH_3)PP$	448	669
$4NP\text{-}H_2TPP$	446	661	$4NP\text{-}H_2T(4\text{-}CH_3)PP$	450	671
$(24DCP)_2H_2T(4\text{-Cl})PP$	448	658	$(24DCP)_2H_2T(4\text{-}CH_3O)PP$	445	688
$4NP\text{-}H_2T(4\text{-Cl})PP$	449	660	$(246TCP)_2H_2T(4\text{-}CH_3O)PP$	454	687
$(24DCP)_2H_2T(4\text{-}CH_3)PP$	449	670	$4NP\text{-}H_2T(4\text{-}CH_3O)PP$	456	695

Table 16. UV-vis peaks (λ/nm in $CHCl_3$) of hydrogen bonded complexes of FBPs with PDs.

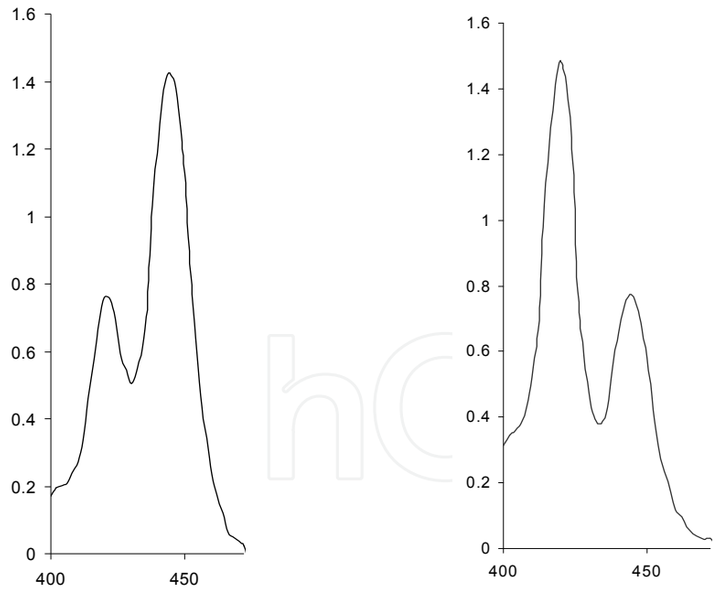

(A) (B)

Fig. 9. In a UV-vis cell a solution of H_2TPP (5×10^{-6} M, 2 ml) and 24DCP (3 M, 90 mic.lit.) at 25 °C (profile A) was cooled to 5 °C (profile B). Observations show that upon cooling the adduct $[(24DCP)_2H_2TPP]$, Soret at 445 nm, has be dissociated to 24DCP and H_2TPP, Soret at 419 nm. By heating of solution to 25 °C the adduct $[(24DCP)_2H_2TPP]$ was formed again and Soret returned to 445 nm.

Stabilities of the adducts increase from $H_2T(4\text{-}Cl)PP$, H_2TPP, $H_2T(4\text{-}CH_3)PP$, to $H_2T(4\text{-}CH_3O)PP$ for each PD, Table 17. For example, at 20 °C we have the following order of the formation constants, *K*:

$(24DCP)_2H_2T(4\text{-}Cl)PP < (24DCP)_2H_2TPP < (24DCP)_2H_2T(4\text{-}CH_3)PP < (24DCP)_2H_2T(4\text{-}CH_3O)PP$

lg K: 1.14 < 1.51 < 1.75 < 1.93

246*TCP* did not show a measurable interaction with H_2TPP and $H_2T(4\text{-}Cl)PP$ under our experimental conditions also its interactions with $H_2T(4\text{-}CH_3)PP$ and $H_2T(4\text{-}CH_3O)PP$ are sizably weaker than corresponding interactions for 24DCP. It might be due to high steric hindrances which coincident to interaction of 246TCP with free base porphyrins. From obtained K for HB complexes the following order could be defined for HB formation ability of PDs: 4NP 〉 24DCP 〉 246TCP

Adduct	lgK				
	5 °C	10 °C	15 °C	20 °C	25 °C
$(24DCP)_2H_2T(4\text{-}Cl)PP$		0.99±0.02	1.08±0.02	1.14±0.02	1.20±0.02
$(24DCP)_2H_2TPP$		1.37±0.01	1.43±0.03	1.51±0.03	1.60±0.03
$(24DCP)_2H_2T(4\text{-}CH_3)PP$		1.58±0.03	1.69±0.04	1.75±0.04	1.86±0.05
$(24DCP)_2H_2T(4\text{-}CH_3O)PP$		1.72±0.01	1.81±0.03	1.93±0.05	2.03±0.02
$(246TCP)_2H_2T(4\text{-}CH_3)PP$		0.67±0.06	0.70±0.05	0.76±0.05	0.80±0.05
$(246TCP)_2H_2T(4\text{-}CH_3O)PP$		0.87±0.02	0.92±0.01	0.99±0.02	1.02±0.02
$(4NP)_2H_2T(4\text{-}Cl)PP$	0.97±0.02	1.09±0.02	1.24±0.02	1.35±0.02	1.44±0.02
$(4NP)_2H_2TPP$	1.02±0.07	1.16±0.05	1.29±0.05	1.47±0.05	1.63±0.08
$(4NP)_2H_2T(4\text{-}CH_3)PP$	1.90±0.02	2.12±0.01	2.35±0.02	2.48±0.02	2.70±0.03
$(4NP)_2H_2T(4\text{-}CH_3O)PP$	1.91±0.01	2.22±0.01	2.40±0.01	2.71±0.02	2.89±0.02

Table 17. The lgK for HB complexes $(PD)_2H_2T(4\text{-}X)PP$ in $CHCl_3$ as solvent.

Thermodynamic parameters ΔH°, ΔS° and ΔG° of $[(PD)_2H_2T(4\text{-}CH_3)PP]$ complexes are given in Table 18. The free energy changes (ΔG°) of HB complexes become more negative through the series $H_2T(4\text{-}Cl)PP$, H_2TPP, $H_2T(4\text{-}CH_3)PP$, to $H_2T(4\text{-}CH_3O)PP$ which indicates stronger HB interaction along this sequence.

Complex	ΔH°	ΔS°	$-\Delta G^\circ$
$(24DCP)_2H_2T(4\text{-}Cl)PP$	19.9±1.8	89.8±6.4	6.9±0.1
$(24DCP)_2H_2TPP$	25.7±2.3	116.7±7.9	9.1±0.1
$(24DCP)_2H_2T(4\text{-}CH_3)PP$	30.1±2.9	136.4±9.9	10.5±0.1
$(24DCP)_2H_2T(4\text{-}CH_3O)PP$	35.2±1.7	156.8±5.8	11.5±0.1
$(246TCP)_2H_2T(4\text{-}CH_3)PP$	15.1±1.4	65.9±4.7	4.5±0.1
$(246TCP)_2H_2T(4\text{-}CH_3O)PP$	17.5±1.3	78.4±4.6	5.9±0.1
$(4NP)_2H_2T(4\text{-}Cl)PP$	38±2	156±5	8±2
$(4NP)_2H_2TPP$	48±2	193±7	9±2
$(4NP)_2H_2T(4\text{-}CH_3)PP$	62±3	260±9	15±3
$(4NP)_2H_2T(4\text{-}CH_3O)PP$	78±4	316±13	17±4

[a] ΔH° ($kJmol^{-1}$), ΔS° ($JK^{-1}mol^{-1}$), ΔG° ($kJmol^{-1}$) at 25°C

Table 18. The thermodynamic parameters for HB complexes $(PD)_2H_2T(4\text{-}X)PP$ in $CHCl_3$[a].

Adducts have positive values of ΔH° and ΔS° but greater contribution of ΔS° relative to ΔH° leads to a negative value of ΔG°.

The positive value of ΔS° may return to association between PDs and free base porphyrin, which accompanied with releasing a greater number of chloroform molecules, that solvated the initial substances. The aggregation between PD and free bases in the selected range of temperatures is endothermic. The following sequence was obtained for interactions of $H_2T(4\text{-}X)PPs$ with phenol derivatives:

$$H_2T(4\text{-}CH_3O)PP > H_2T(4\text{-}CH_3)PP > H_2TPP > H_2T(4\text{-}Cl)PP$$

4. Effect of nonplanarity of free base porphyrins on their interactions with dimethyl- and diethyltin(IV) dichlorides

The nonplanarity of the free base porphyrin can be regulated by electronic and steric effects of the *meso*- and β-pyrrole substitution and it has profound consequences on spectral, electrochemical, and other properties of porphyrins. [45-48] Chemical properties that are known to be modified by nonplanar distortion include oxidation potentials, basicity of the inner nitrogen atoms, and axial ligand binding affinity, all of which can influence the biological function of porphyrin cofactors in proteins. A good result of nonplanar distortion of porphyrins appears in porphyrin metalation. For example, the predeformed octabromo-tetramesityl-porphyrin incorporates Zn^{2+} about 4000 times faster than the planar tetramesityl-porphyrin in DMF with the same rate law. Since the rates of metal ion incorporation are attributed to the conformational change of the rigid planar porphyrin core, thus the metalation of a nonplanar porphyrin is distinct in reaction rate from that of planar porphyrins.

This fact has be pointed out that nonplanarity enhances the basicity of porphyrins. This part do to comparison of the acceptor property of nonplanar *meso*-tetrakis-tert-butylporphyrin (H_2TtBP) with planar *meso*-tetra-n-propylporphyrin (H_2TnPP), in their interactions with dimethyl- and diethyltin(IV) dichloride.

On mixing of the R_2SnCl_2 (R= Me, Et) with a solution of free bases H_2TnPP and H_2TtBP Lewis acid-base interactions were occurred between them.[49] Porphyrins as Lewis bases coordinated to organotin compounds as Lewis acids. Extent of these interactions depends on acid-base properties of interacting components.

4.1 ^{1}H NMR analysis

The ^{1}H NMR spectra of porphyrins moiety in these adducts show clear differences relative to the free bases reactants. Upon complexation of free base porphyrins with organotin(IV) halides the H_β of pyrrole rings (H_2TnPP 9.5 and H_2TtBP 9.08 ppm) were shifted up field (9.03 and 8.1 ppm, respectively) while the N-H pyrrolic protons (H_2TnPP -2.6 and H_2TtBP 1.52 ppm) show down field shift and collapsed with alkyls protons at chemical shifts 1-2.5 ppm. These variations in ^{1}H NMR spectra result from enhancement of nonplanar distortion in porphyrin structure during adduct formation. Comparison of chemical shifts of ^{1}H NMR of free bases H_2TnBP and H_2TtBP especially for NH protons clearly shows the effect of nonplanarity on the ^{1}H NMR of free base porphyrins. In the 5,10,15,20-tetrabutylporphyrin (H_2TnBP) as a planar porphyrin the N-H and H_β signals were appeared at -2.61 and 9.45

ppm, respectively, while in the 5,10,15,20-tetrakis(tert-butyl)porphyrin (H_2TtBP) as a severely distorted porphyrin the N-H and H_β were appeared at 1.52 and 9.08 ppm.

4.2 UV-vis analysis

4.2.1 Interactions of R_2SnCl_2 with H_2TnPP

By interaction of R_2SnCl_2 with H_2TnPP Soret band of free base porphyrin (original peak at 417 nm) was shifted to 433 nm, see Table 19 and Fig.9. In addition other peaks of H_2TnPP were weakened while a new peak was appeared at 643 nm. Presence of a clear isosbestic point at 425 nm can aroused from an equilibrium in solution.

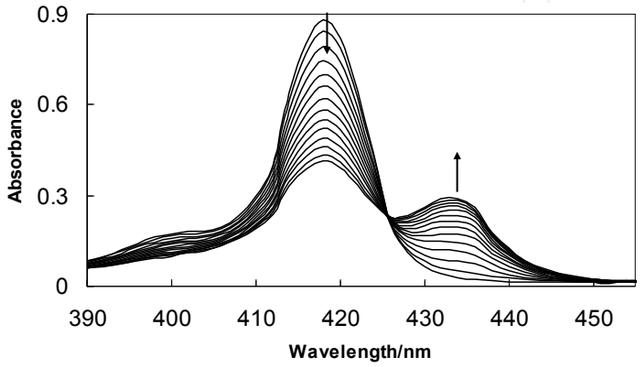

Fig. 9. Titration spectra for titration of H_2TnPP with Et_2SnCl_2 in chloroform. Band appeared at 433 nm is related to adduct, isosbestic points at 425 nm.

Compound	λ (nm)					Compound	λ (nm)				
H_2TnPP	417	520	555	600	659	H_2TtBP	446	552	596	628	691
$(Me_2SnCl_2)_2H_2TnPP$	433	-	-	-	643	$(Me_2SnCl_2)_2H_2TtBP$	453	-	-	-	695
$(Et_2SnCl_2)_2H_2TnPP$	433	-	-	-	643	$(Et_2SnCl_2)_2H_2TtBP$	453	-	-	-	695

Table 19. UV-vis peaks of free base porphyrins and their adducts with R_2SnCl_2 in $CHCl_3$.

4.2.2 Interaction of R_2SnCl_2 with H_2TtBP

By interaction of R_2SnCl_2 with H_2TtBP, the Soret band of free base porphyrin (original peak at 446 nm) was shifted to 453 nm, see Table 19 and Fig. 10. In addition, other peaks of H_2TtBP were weakened while a new peak was appeared at 695 nm. Presence of a isosbestic point at 454 nm can be argued by existence of equilibrium in solution.

Amount of replacement of Soret band in H_2TnPP (16 nm) is greater than H_2TtBP (7 nm). This aroused from greater nonplanar distortion in H_2TnPP skeleton comparing to H_2TtBP during adduct formation. Since the observed red shift mainly depends on the distortion of porphyrins structures during adduct formations.

For practical illustration of this subject, if in a batched UV-vis cell at 5 °C, a solution of H_2TnPP titrated with Me_2SnCl_2 the Soret band of free base (417 nm) will diminish and Soret band related to adduct will appear at 433 nm. By keeping the composition of solution unchanged and raising the temperature to 35 °C the Soret band will go back to 417 nm. This phenomenon which could be repeated successively shows that adduct dissociate to Me_2SnCl_2 and H_2TnPP at elevated temperatures and forms on cooling in equilibrium.

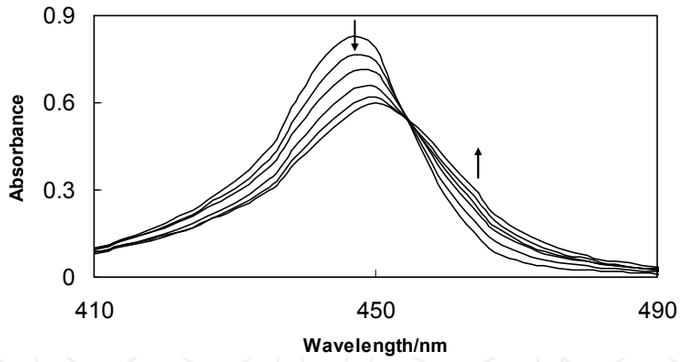

Fig. 10. Titration spectra, for titration of H_2TtBP with Me_2SnCl_2 in chloroform. Band appeared at 453 nm is related to adduct, isosbestic point at 454 nm.

About 20-30 nm red shift have been observed for Soret band of porphyrin moiety in the complexes of tetraarylporphyrins with organotin(IV) halides. A similar situation but with smaller red shifts (16 and 7 nm) were observed for interaction of H_2TnPP and H_2TtBP with R_2SnCl_2. Of course, with a considerable resonance that there is between peripheral aryl rings and porphyrin core in tetraarylporphyrins and lack of such resonance in tetraalkyl porphyrins this difference will be reasonable. Generally, porphyrin distortion is accompanied by bathochromic shift of its electronic absorption bands. [24,26] For example, in UV-vis spectra (in CH_2Cl_2) of planar porphyrin H_2TnPP Soret band and Q bands were observed at (417 nm) and (520, 555, 600, 659 nm), respectively. But in distorted H_2TtBP, Soret band and Q bands appeared at (446 nm) and (552, 596, 628, 691 nm). The effect of distortion of porphyrin plane on electronic absorption and ^1H NMR spectra of the free base porphyrin clearly observed from these data. Thus in these adducts greater red shifts in the UV-vis spectra of H_2TnPP may be due to more distortions in its structure during adduct formations.

4.3 Thermodynamic studies

The data given in Table 20 show that formation constants for adducts of H_2TtBP with dimethyl- and diethyltin(IV) dichloride are greater than related values for H_2TnPP. It shows that $(R_2SnCl_2)_2H_2TtBP$ adducts are more stable than $(R_2SnCl_2)2H_2TnPP$. For example at 5 °C we have the following order of the formation constants:

$$(Me_2SnCl_2)_2H_2TtBP > (Me_2SnCl_2)_2H_2TnPP; \quad \lg K \ 9.70 > 6.58$$

$$(Et_2SnCl_2)_2H_2TtBP > (Et_2SnCl_2)_2H_2TnPP; \quad \lg K \ 8.35 > 5.69$$

Also comparison of stability constants show that Me_2SnCl_2 adducts are more stable than their Et_2SnCl_2 counterparts.

$$(Me_2SnCl_2)_2H_2TnPP > (Et_2SnCl_2)_2H_2TnPP; \quad \lg K \ 6.58 > 5.69$$

$$(Me_2SnCl_2)_2H_2TtBP > (Et_2SnCl_2)_2H_2TtBP; \quad \lg K \ 9.70 > 8.35$$

Table 21 shows the thermodynamic parameters obtained for the interactions of R_2SnCl_2 with free base porphyrins in chloroform. Adducts have negative values of ΔH°, ΔS°, and ΔG°. The negative values of ΔS° refer to association between donor and acceptor molecules.

Adduct	lgK				
	5 °C	10 °C	15 °C	20 °C	25 °C
$(Me_2SnCl_2)_2H_2TnPP$	6.58±0.02	6.17±0.01	5.72±0.01	5.30±0.04	4.90±0.01
$(Et_2SnCl_2)_2H_2TnPP$	5.69±0.02	5.33±0.03	4.84±0.09	4.52±0.04	4.18±0.01
$(Me_2SnCl_2)_2H_2TtBP$	9.70±0.01	9.15±0.01	8.66±0.09	8.01±0.03	7.51±0.02
$(Et_2SnCl_2)_2H_2TtBP$	8.35±0.02	7.87±0.02	7.52±0.09	7.11±0.02	6.73±0.04

Table 20. The formation constants (lg K) of adducts in $CHCl_3$.

Adduct	$-\Delta H^o$	$-\Delta S^o$	$-\Delta G^o$
$(Me_2SnCl_2)_2H_2TnPP$	134 ±1	356 ±5	28 ±1
$(Et_2SnCl_2)_2H_2TnPP$	121 ±4	328 ±40	24 ±4
$(Me_2SnCl_2)_2H_2TtBP$	170 ±6	426 ±20	43 ±20
$(Et_2SnCl_2)_2H_2TtBP$	123 ±2	284 ±5	39 ±2

[a] ΔH^o ($kJmol^{-1}$), ΔS^o ($JK^{-1}mol^{-1}$), and ΔG^o at 10 °C ($kJmol^{-1}$).

Table 21. The thermodynamic parameters of adducts in $CHCl_3$.[a]

Both free energy and enthalpy of adducts of H_2TtBP are more negative than corresponding values for H_2TnPP. This indicates that interactions of H_2TtBP with organotin compounds are stronger than H_2TnPP. This trend is in according to the electron donation of the free base porphyrins. Since, in the pre-distorted H_2TtBP lone pair electrons of nitrogen atoms are more ready for coordination to R_2SnCl_2 Lewis acid. Therefore, we found greater formation constants for complexes of R_2SnCl_2 with H_2TtBP than H_2TnPP.

5. References

[1] N. Zh. Mamardashvili, O A Golubchikov, *Russian Chemical Reviews*, 70 (2001) 577 and references there in.

[2] H Ogoshi, E-i Watanabe, N Koketsu, Z-i Yoshida, *Bull. Chem. Soc. Jpn.*, 49 (1976) 2529.

[3] N. Datta-Gupta, T. J. Bardos, *J. Heterocycl. Chem.*, 3 (1966) 495.

[4] E.B. Fleischer and J.H. Wang, *J. Am. Chem. Soc.*, 82 (1960) 3498.

[5] F.R. Longo, E.M. Brown, W.G. Rau, and A.D. Alder in "*The Porphyrins*" Vol. V, D. Dolphin, Ed., Academic Press, New York, 1979, pp 459.

[6] Funahashi, S., Yamaguchi, Y., Tanaka, M., *Bull. Chem. Soc. Jpn.*, 57 (1984) 204.

[7] Funahashi, S., Yamaguchi, Y., Tanaka, M., *Inorg. Chem.*, 23 (1984) 2249.

[8] Robinson, L. R.; Hambright, P., *Inorg. Chim. Acta*, 185 (1991) 17.

[9] Bain-Ackerman, M. J.; Lavallee, D. K., *Inorg. Chem.*, 18 (1979) 3358.

[10] Funahashi, S.; Saito, K.; Tanaka, M., *Bull. Chem. Soc. Jpn.*, 54 (1981) 2695.

[11] Pasternack, R. F., Vogel, G. C., Skowronek, C. A., Harris, R. K., Miller, J. G., *Inorg. Chem.*, 20 (1981) 3763.

[12] Hambright, P. and Chock, P. B., *J. Am. Chem. Soc.*, 96 (1974) 3123.

[13] Turay, J., Hambright, P., *Inorg. Chem.*, 19 (1980) 562.

[14] Fleischer, E. B., Dixon, F., *Bioinorg. Chem.*, 7 (1977) 129.

[15] S. Funahashi, M. Inamo, N. Kamiya, Y. Inada, M. Nomura, *Inorg. Chem.*, 40 (2001) 5636.

[16] S. Funahashi, Y. Inada, Y. Sugimoto, Y. Nakano, Y. Itoh, *Inorg. Chem.*, 37 (1998) 5519.
[17] M. Asadi, A. Zabardasti, J. Ghasemi, Polyhedron 21 (2002) 683.
[18] M. Asadi, A. Zabardasti, J. Ghasemi, *Bull. Chem. Soc. Jpn.,75 (2002)1137.*
[19] M. Asadi, A. Zabardasti, *J. Chem. Research (S)* 2002, 611.
[20] A. Zabardasti1, M. Salehnassaje, M. Asadi, V.A. Karimivand, *Polish J. Chem.*, 80 (2006) 1473.
[21] M Asadi, A. Zabardasti, V. A. Karimivand, J. Ghasemi, Polyhedron 21 (2002) 1255.
[22] A. Zabardasti, M. Asadi, A. Kakanejadifard, *J. Heterocyclic Chem.*, 43 (2006) 1157.
[23] A. Zabardasti, M. Asadi, V.A. Karimivand and J. Ghasemi, *Asian J. Chem.*, 17 (2005) 711.
[24] E.B. Fleischer and A.L. Stone, *Chem. Soc. Chem. Commu*. 332 (1967).
[25] B. Cheng, O. Q. Munro, H. M. Marques, and W. R. Scheidt, *J. Am. Chem. Soc.*, 119 (1997) 10732.
[26] M.O. Senge, I. Bischoff, N.Y. Nelson, K.M. Smith, *J. Porphyrins Phthalocyanines*, 3 (1999) 99.
[27] Storm, C. B.; Teklu, Y., *J. Am. Chem. Soc.*, 94 (1972) 1745.
[28] Storm, C. B.; Teklu, Y.; Sokoloski, A. *Ann. N. Y. Acad. Sci.*, 206 (1973) 631.
[29] K.M.Smith and M.F.Hudson, *Tetrahedron*, 32 (1976) 597.
[30] P. Worthington, P. Hambright, R.F.X. Williams, J. Reid, C. Burnham, A. Shamim, J. Turay, D.M. Bell, R. Kirkland, R.G. Little, N. Datta-Gupta, and E. Eisner, *J. Inorg. Biochem.*, 12 (1980) 281.
[31] D.J. Leggett, "*Computational Methods for the Determination of Formation Constant*", Plenum Press, New York, 1985.
[32] R.S. Mulliken, W.B. Person, *Molecular Complexes: A Lecture and Reprint*, John Wiley and Sons: New York; 1969.
[33] N. Haga,; H. Nakajima, H. Takayanagi, K. Tokumaru, *J. Org. Chem.*, 63 (1998) 5372.
[34] H. Dehghani, M. Babaahmadi, *Polyhedron*, 27 (2008) 2739.
[35] H. Dehghani, M. Babaahmadi, *Polyhedron*, 27 (2008) 2416.
[36] A. Zabardasti, M. Mirzaeian, *Chem. Lett.*, 35 (2006) 1348.
[37] A. Zabardasti, M. Mirzaeian, *Asian J. Chem.*, 19 (2007) 4753.
[38] A. Zabardasti, L. Shaebani, A. Kakanejadifard, F. Faragi Morchegani, Bull. Chem. Soc. Ethiop., 25 (2011) 127.
[39] L. Guilleux, P. Krausz, L. Nadjo, C. Giannotti, R. Uzan, J. Chem. Soc. Perkin Trans. II (1984) 475.
[40] K. Kano, S. Hashimoto, Bull. Chem. Soc. Jpn. 63 (1990) 633.
[41] K. Kano, T. Hayakawa, S. Hashimoto, Bull. Chem. Soc. Jpn. 64 (1991) 778.
[42] D. Mohajer, H. Dehghani, J. Chem. Soc. Perkin Trans. II (2000) 199.
[43] A. Zabardasti, S. Farhadi, Z. Rezvani-Abkenari, Asian J. Chem., 19 (2007) 5488.
[44] A. Zabardasti, Z. Rezvani-Abkenari, *J. Iran. Chem. Soc.*, 5 (2008) 57.
[45] E.I. Sagun, E.I. Zenkevich, V.N. Knyukshto, A.M. Shulga, D.A. Starukhin, C. von Borczyskowski, *Chem. Phys.*, 275 (2002) 211.
[46] C.K. Mathews, K.E. Van Holde, K.G. Ahern, *Biochemistry*, Addison, Wesley Longman, San Francisco, 2000.
[47] B.O. Fernandez, I.M. Lorkovic and P.C. Ford, *Inorg. Chem.*, 43 (2004) 5393.

[48] P.D. Beer, D.P. Cormode and J.J. Davis, *Chem. Commun.*, (2004) 414.
[49] A. Zabardasti, S. Farhadi, M.H. Rahmati, J. Chem. Research, (2010) 538.

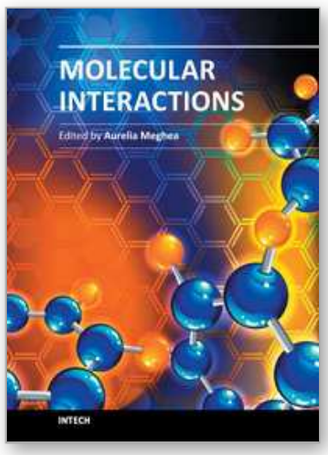

Molecular Interactions

Edited by Prof. Aurelia Meghea

ISBN 978-953-51-0079-9
Hard cover, 400 pages
Publisher InTech
Published online 29, February, 2012
Published in print edition February, 2012

In a classical approach materials science is mainly dealing with interatomic interactions within molecules, without paying much interest on weak intermolecular interactions. However, the variety of structures actually is the result of weak ordering because of noncovalent interactions. Indeed, for self-assembly to be possible in soft materials, it is evident that forces between molecules must be much weaker than covalent bonds between the atoms of a molecule. The weak intermolecular interactions responsible for molecular ordering in soft materials include hydrogen bonds, coordination bonds in ligands and complexes, ionic and dipolar interactions, van der Waals forces, and hydrophobic interactions. Recent evolutions in nanosciences and nanotechnologies provide strong arguments to support the opportunity and importance of the topics approached in this book, the fundamental and applicative aspects related to molecular interactions being of large interest in both research and innovative environments. We expect this book to have a strong impact at various education and research training levels, for young and experienced researchers from both academia and industry.

INTECH
open science | open minds

InTech Europe
University Campus STeP Ri
Slavka Krautzeka 83/A
51000 Rijeka, Croatia
Phone: +385 (51) 770 447
Fax: +385 (51) 686 166
www.intechopen.com

InTech China
Unit 405, Office Block, Hotel Equatorial Shanghai
No.65, Yan An Road (West), Shanghai, 200040, China
中国上海市延安西路65号上海国际贵都大饭店办公楼405单元
Phone: +86-21-62489820
Fax: +86-21-62489821

IntechOpen